Magnetism as seen with X-Rays

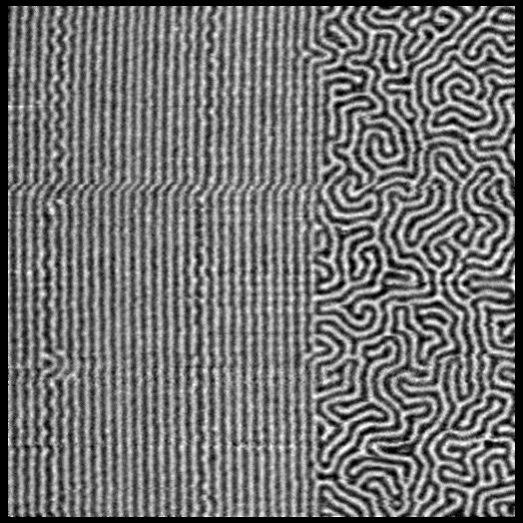

Elke Arenholz

Lawrence Berkeley National Laboratory

and

Department of Material Science and Engineering, UC Berkeley

Magnetic Materials Today

Magnetic materials
for
energy applications

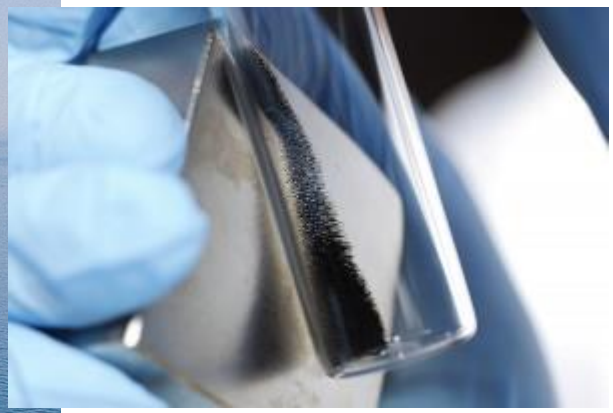

Magnetic
nanoparticles
for
biomedical and
environmental
applications

Magnetic thin films
for
information storage
and processing

Magnetic Materials Characterization Wish List

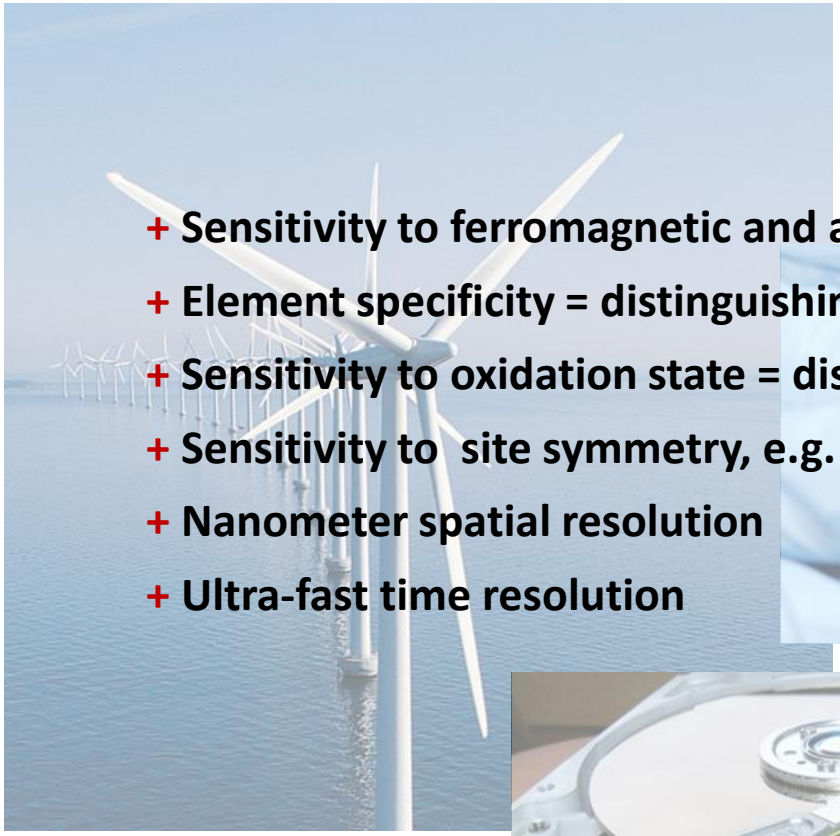

+ Sensitivity to ferromagnetic and antiferromagnetic order
+ Element specificity = distinguishing Fe, Co, Ni, …
+ Sensitivity to oxidation state = distinguishing Fe^{2+}, Fe^{3+}, …
+ Sensitivity to site symmetry, e.g. tetrahedral, $T_{d;}$ octahedral, O_h
+ Nanometer spatial resolution
+ Ultra-fast time resolution

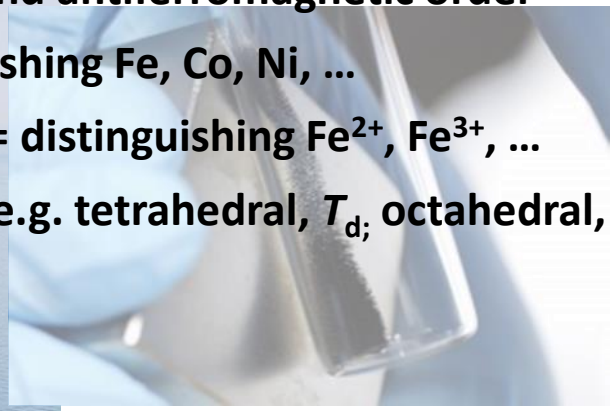

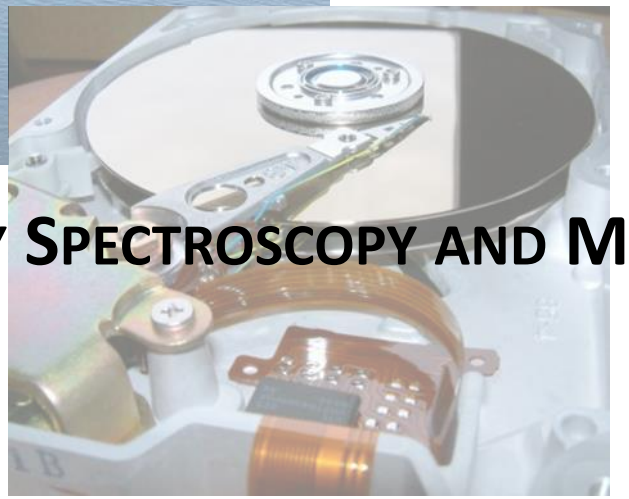

Soft X-Ray Spectroscopy and Microscopy

SPECTROSCOPY

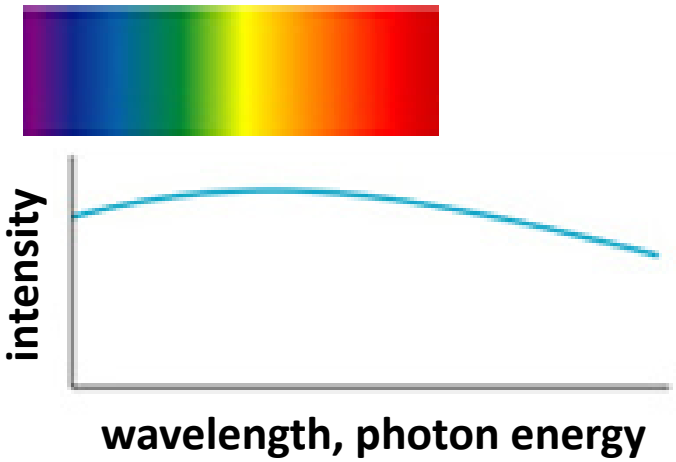

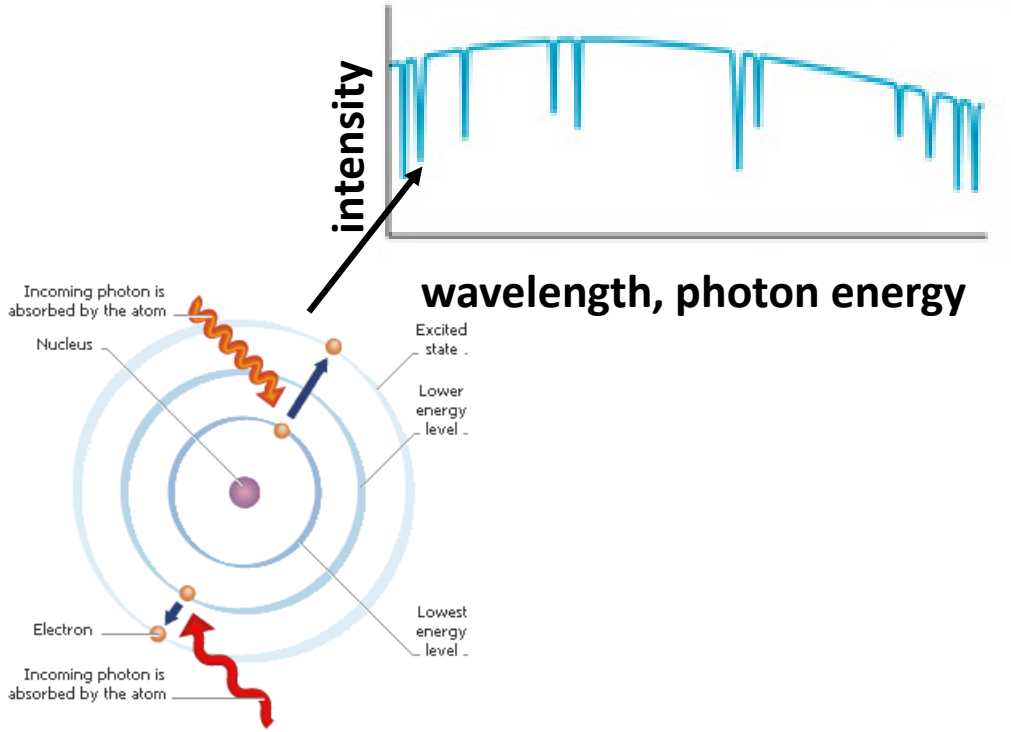

Soft X-Ray Spectroscopy (hν ≈ 500-1000eV, λ ≈ 1-2nm)

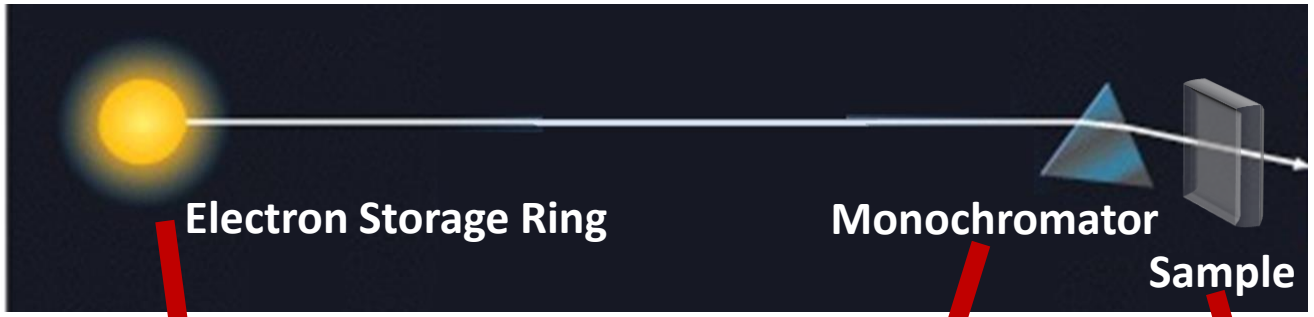

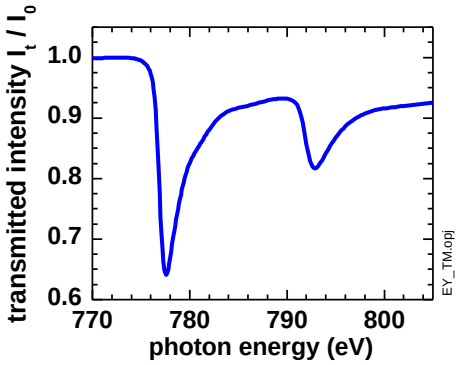

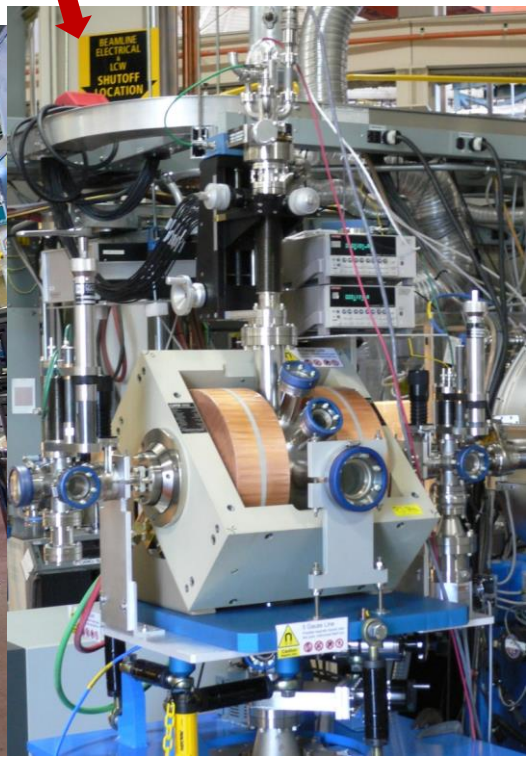

X-Ray Absorption – Detection Modes

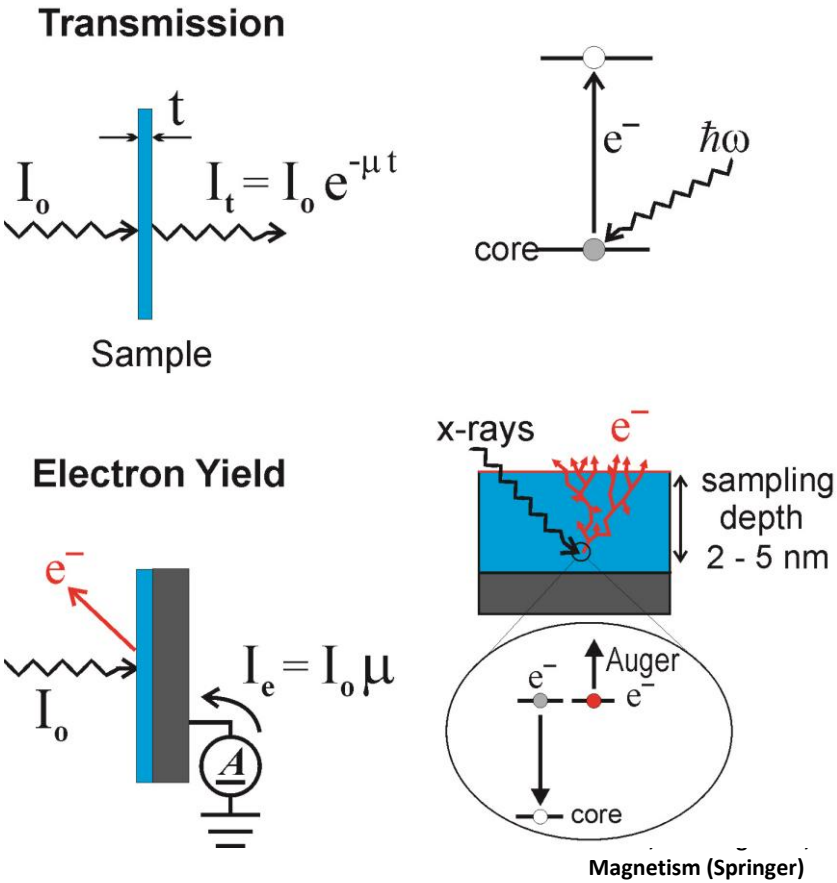

Magnetism (Springer)

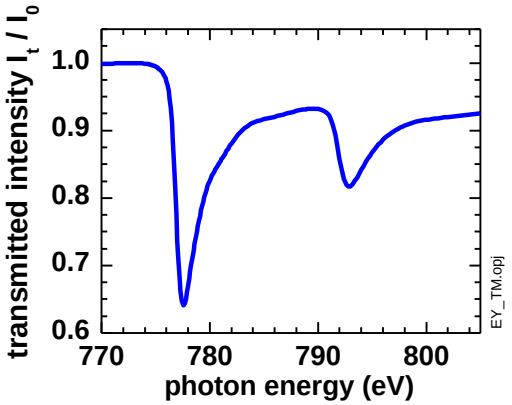

photons absorbed

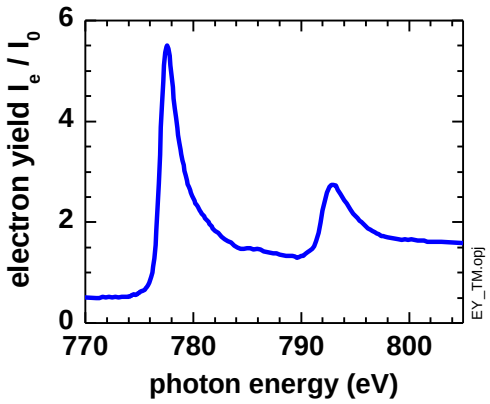

electrons generated

Electron yield:

+ Absorbed photons create core holes subsequently filled by Auger electron emission
+ Auger electrons create low-energy secondary electron cascade through inelastic scattering
+ Emitted electrons ∝ probability of Auger electron creation ∝ absorption probability

Soft X-Ray Absorption – Probing Depth

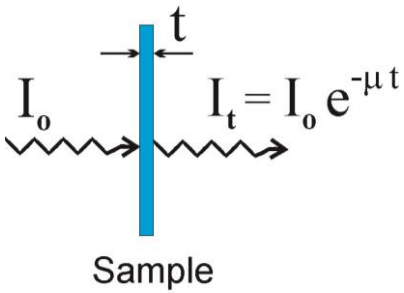

Element	10eV below L_3 1/μ [nm]	at L_3 1/μ [nm]	40 eV above L_3 1/μ [nm]
Fe	550	17	85
Co	550	17	85
Ni	625	24	85

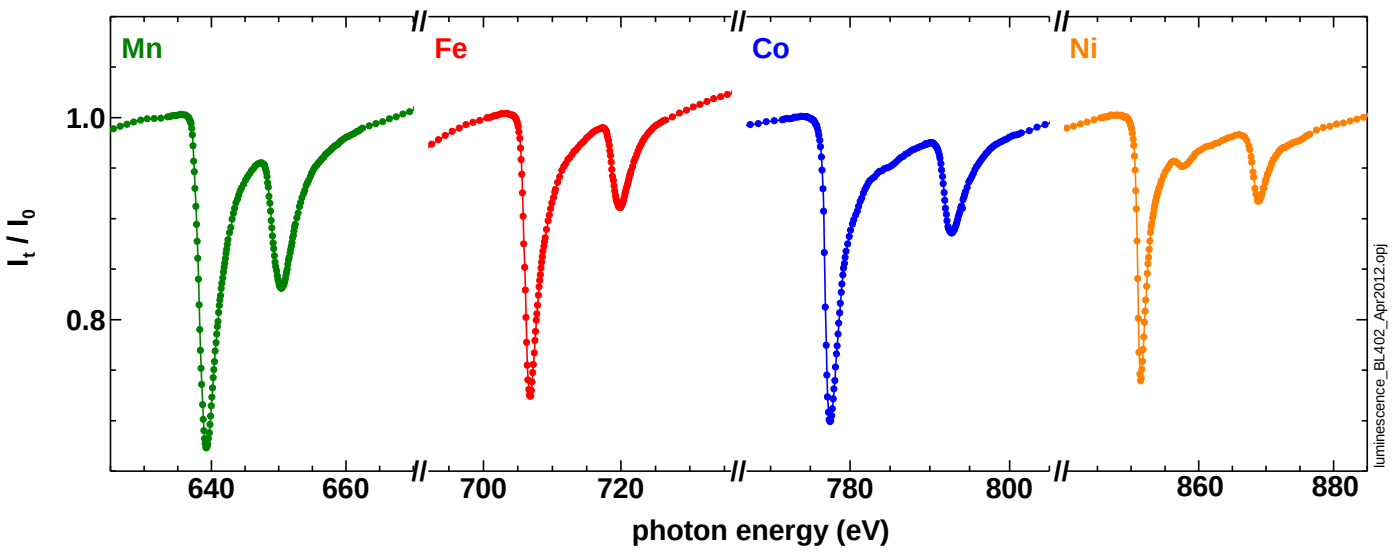

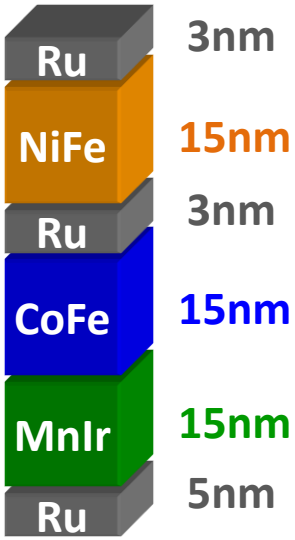

~10-20 nm layer thick films supported by substrates transparent to soft x-rays

X-Ray Absorption – Detection Modes and Probing Depth

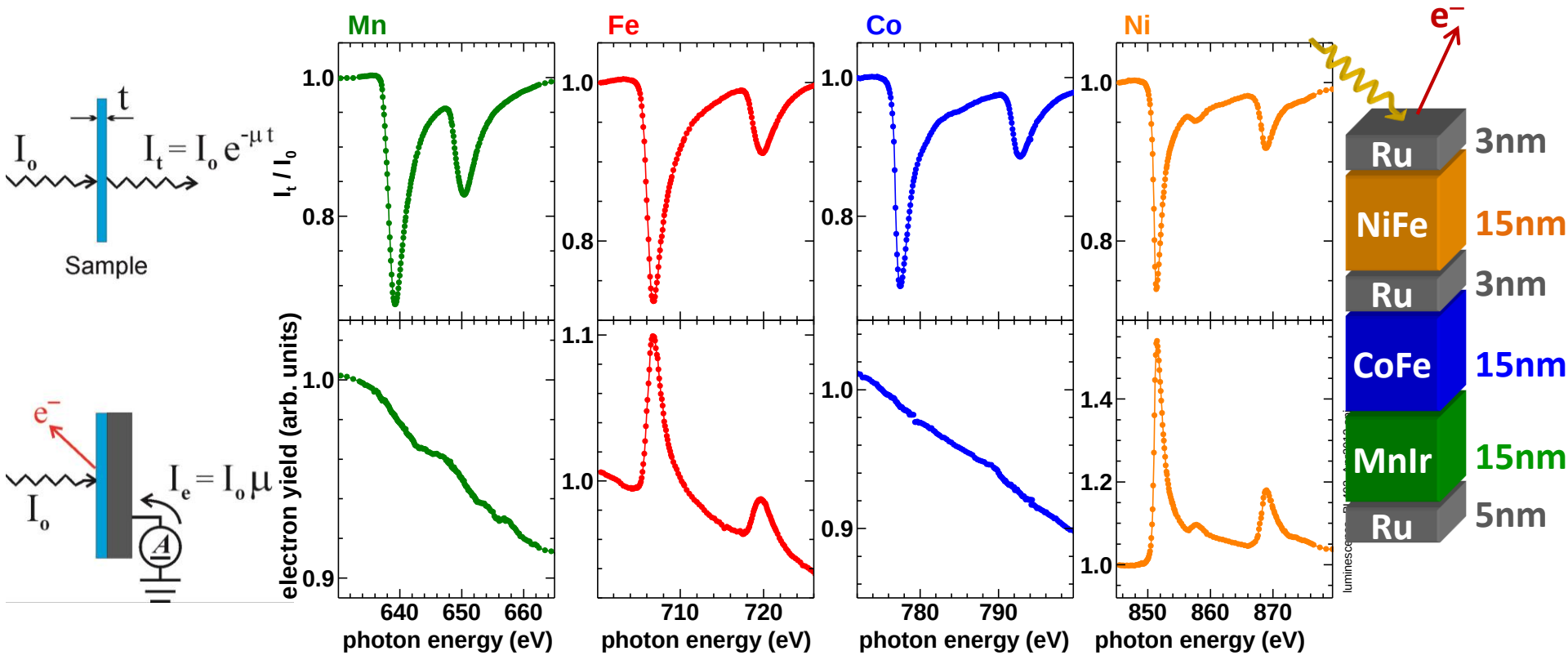

+ **Electron sample depth: 2-5 nm in Fe, Co, Ni**

  ⇒ **60% of the electron yield originates form the topmost 2-5 nm**

X-Ray Absorption – Fundamentals

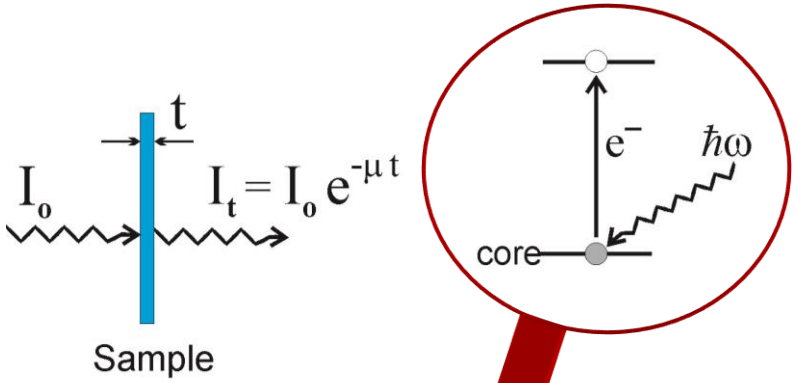

Experimental Concept:

Monitor reduction in x-ray flux transmitted through sample as function of photon energy

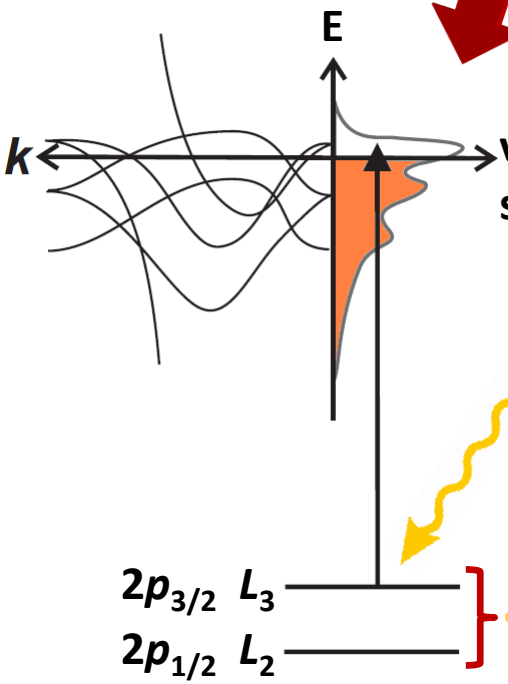

⇒ charge state of absorber Fe^{2+}, Fe^{3+}

⇒ symmetry of lattice site of absorber: O_h, T_d

⇒ sensitive to magnetic order

⇒ Absorption probability: x-ray energy, x-ray polarization, experimental geometry

core level ⇒ atomic species of absorber Fe, Co, Ni, ….

'White Line' Intensity

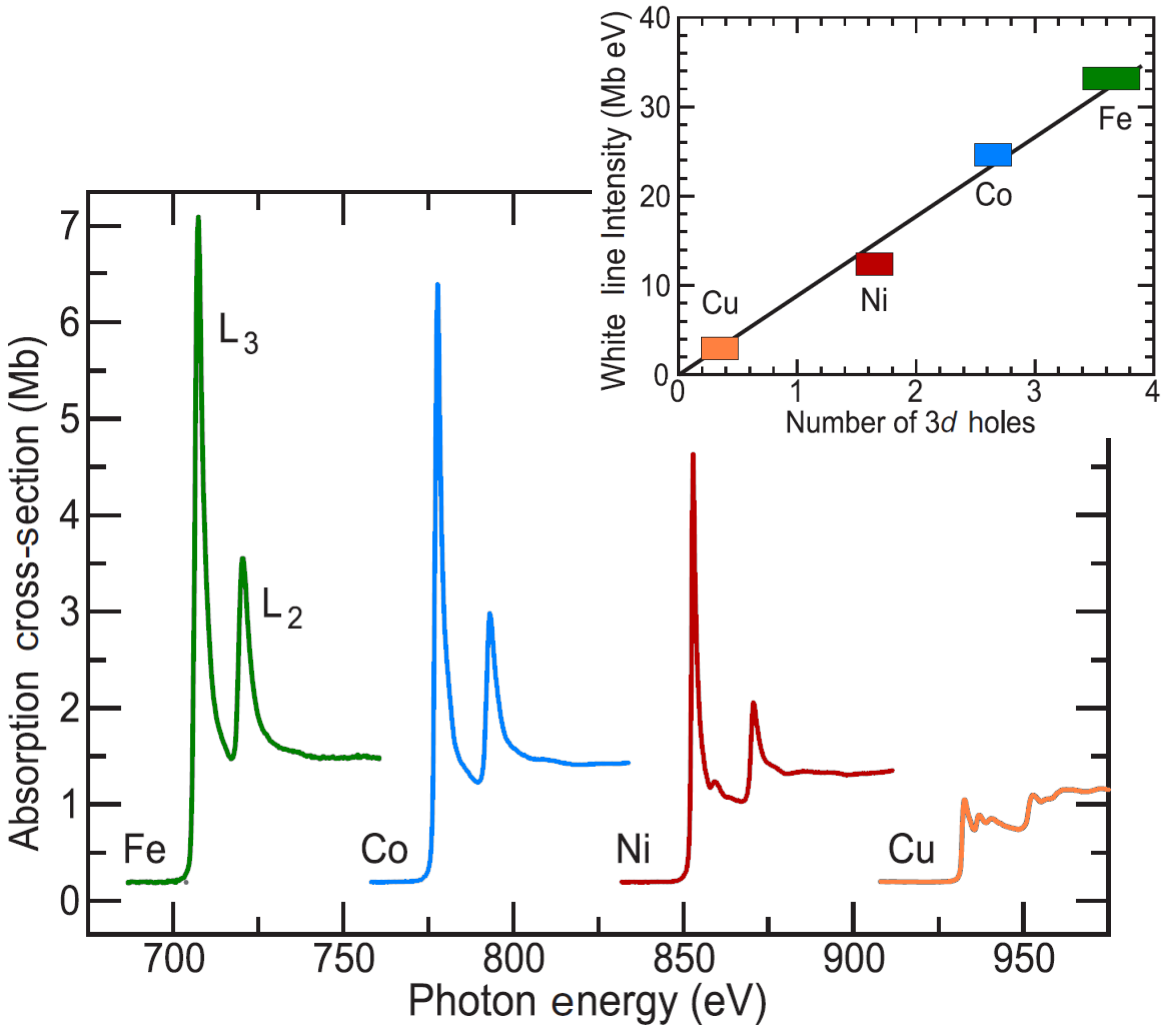

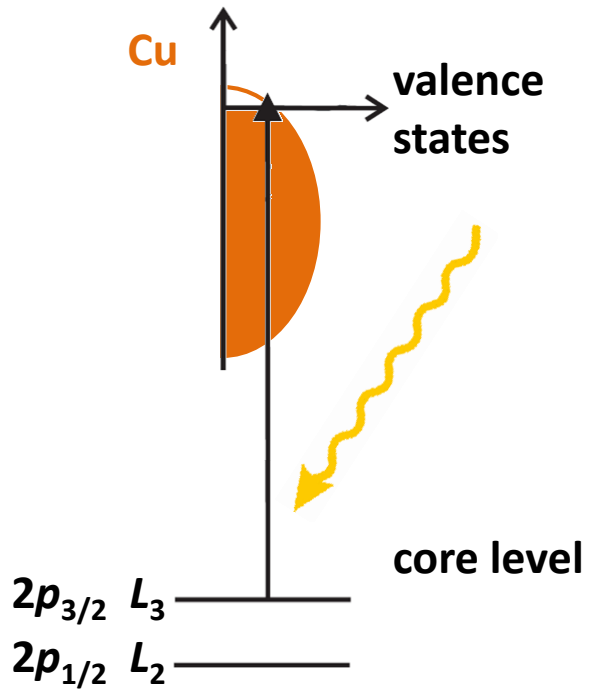

Intensity of $L_{3,2}$ resonances is proportional to number of *d* states above the Fermi level, i.e. number of holes in the *d band.*

X-Ray Absorption – Fundamentals

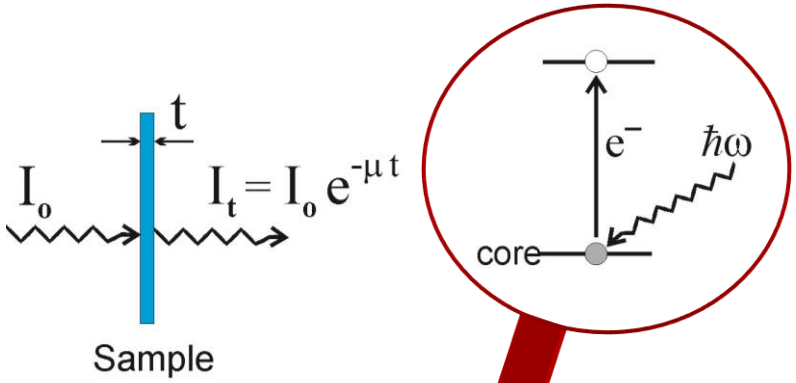

Experimental Concept:

Monitor reduction in x-ray flux transmitted through sample as function of photon energy

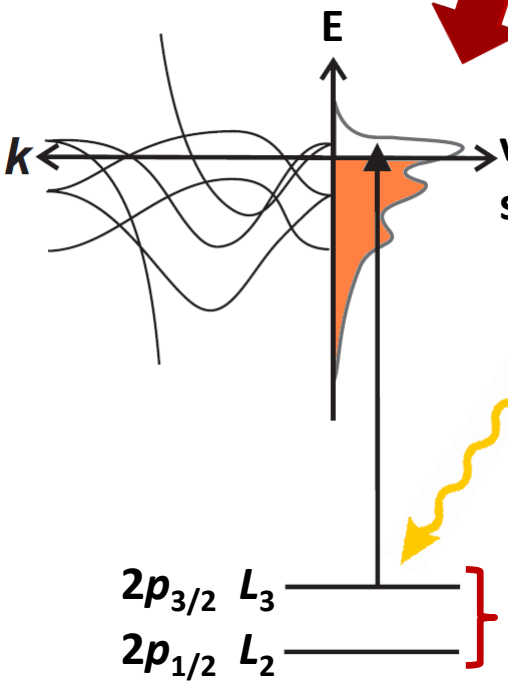

⇒ charge state of absorber Fe^{2+}, Fe^{3+}, …

⇒ symmetry of lattice site of absorber: O_h, T_d

⇒ sensitive to magnetic order

⇒ Absorption probability: x-ray energy, x-ray polarization, experimental geometry

core level ⇒ atomic species of absorber Fe, Co, Ni, ….

X-RAY ABSORPTION – VALENCE STATE

Influence of the charge state of the absorber

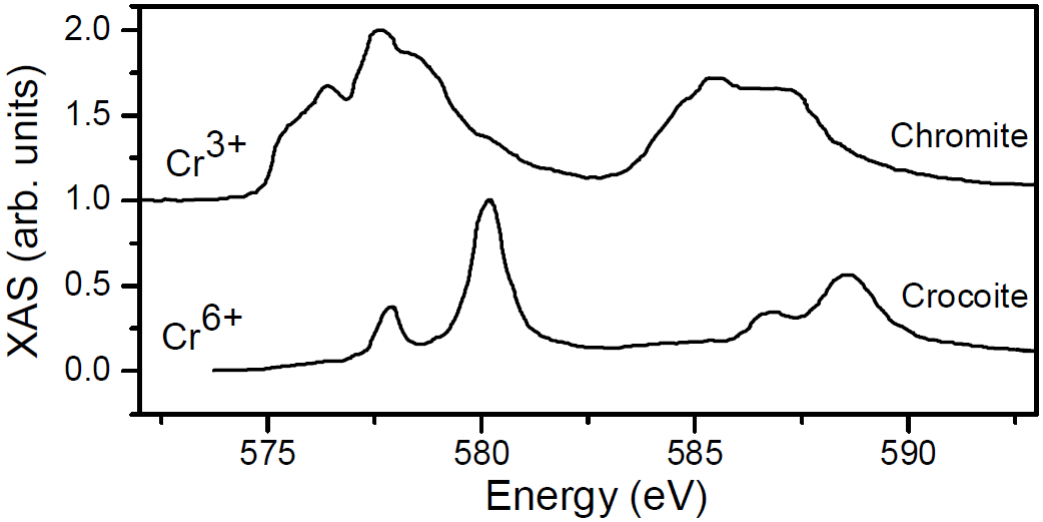

N. Telling *et al.*,
Appl. Phys. Lett. 95, 163701 (2009)

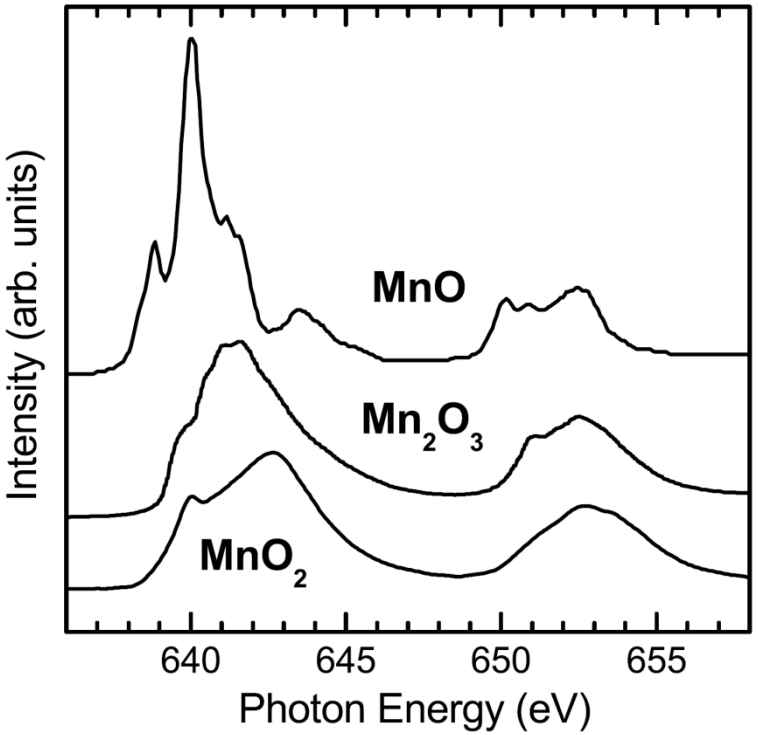

J.-S. Kang et al., Phys. Rev. B 77, 035121 (2008)

X-Ray Absorption – Configuration Model

Ni^{2+} in NiO: $2p^6\ 3d^8 \rightarrow 2p^5\ 3d^9$

Configuration model, e.g. *L* edge absorption :

- **Excited from ground/initial state configuration, $2p^6 3d^8$ to exited/final state configuration, $2p^5 3d^9$**
- **Omission of all full subshells (spherical symmetric)**
- **Takes into account correlation effects in the ground state as well as in the excited state**
- **Leads to multiplet effects/structure**

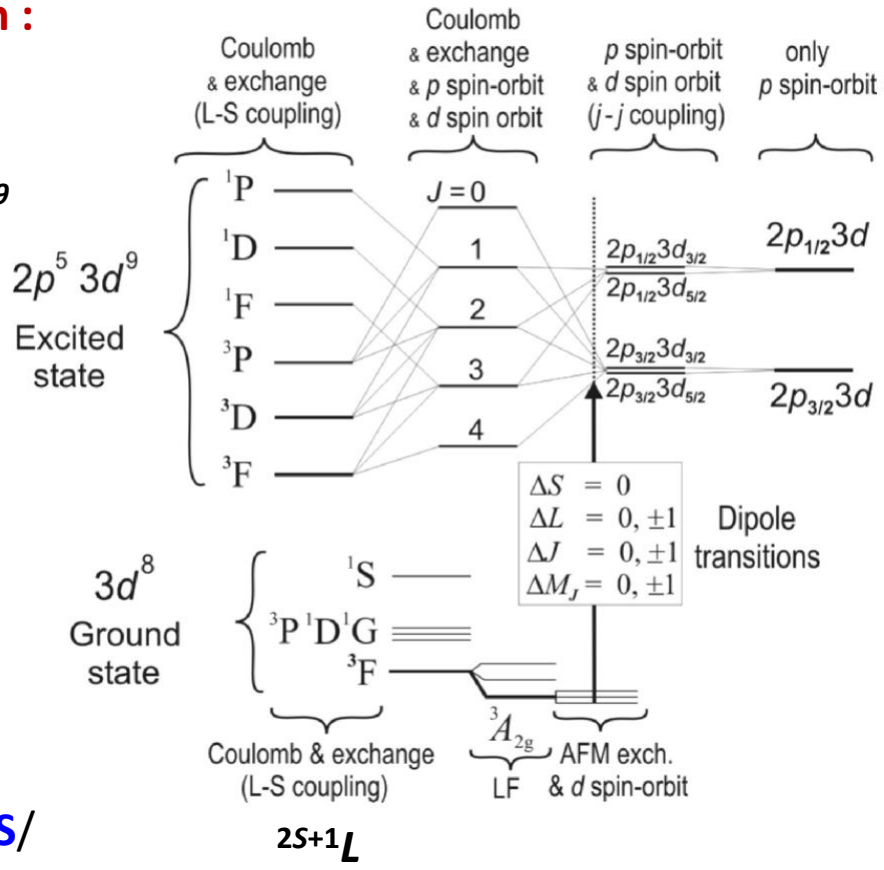

http://www.anorg.chem.uu.nl/CTM4XAS/

J. Stöhr, H.C. Siegmann, Magnetism (Springer)

X-Ray Absorption – Fundamentals

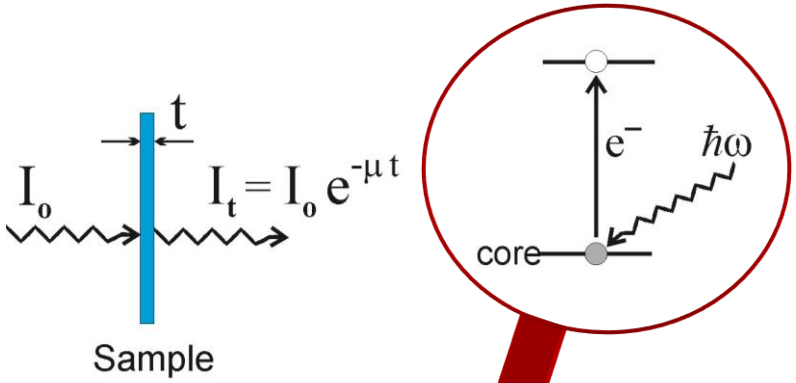

Experimental Concept:

Monitor reduction in x-ray flux transmitted through sample as function of photon energy

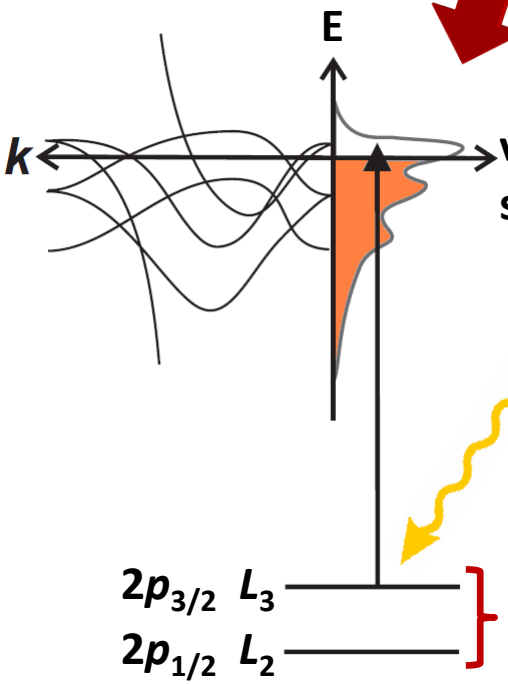

⇒ charge state of absorber Fe^{2+}, Fe^{3+}

⇒ symmetry of lattice site of absorber: O_h, T_d

⇒ sensitive to magnetic order

⇒ Absorption probability: x-ray energy, x-ray polarization, experimental geometry

core level ⇒ atomic species of absorber Fe, Co, Ni, ….

Sensitivity To Site Symmetry: Ti^{4+} $L_{3,2}$

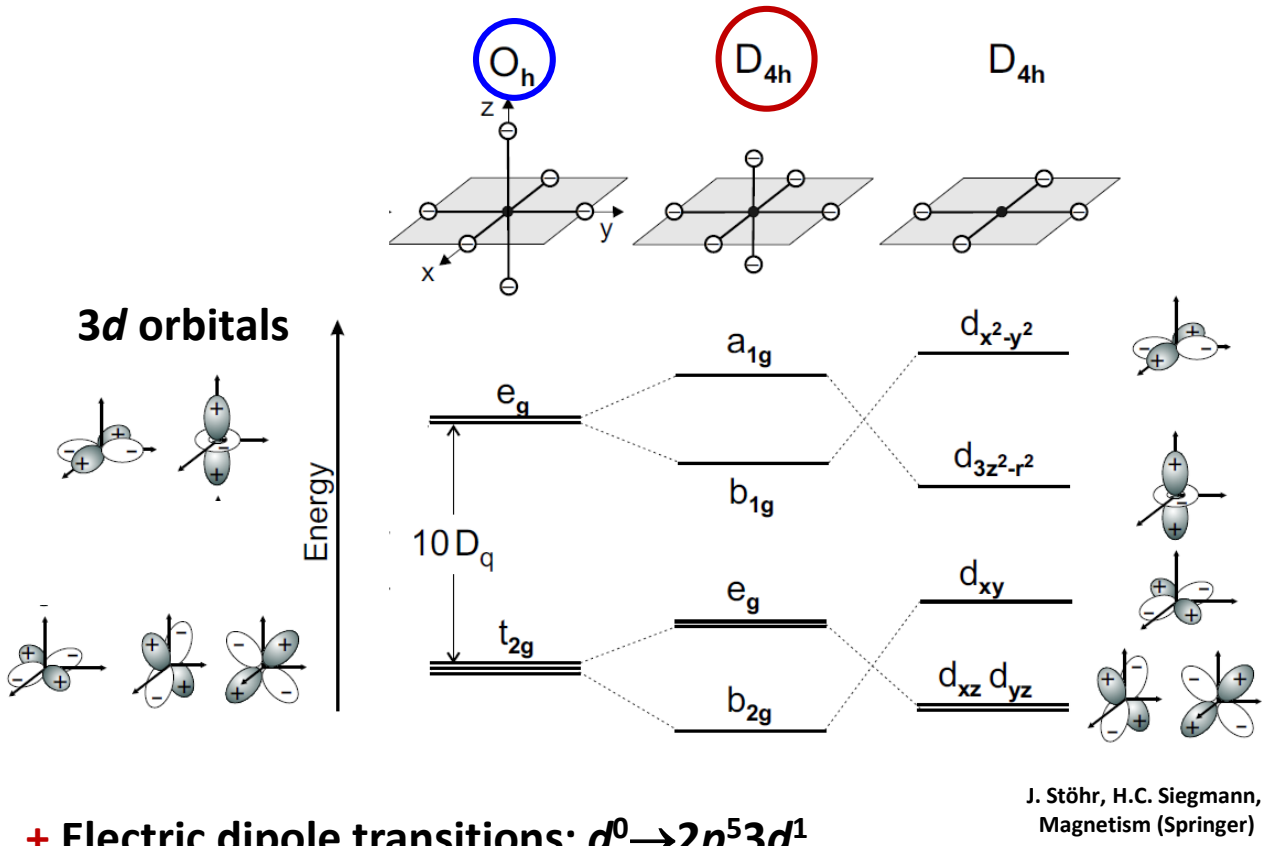

J. Stöhr, H.C. Siegmann, Magnetism (Springer)

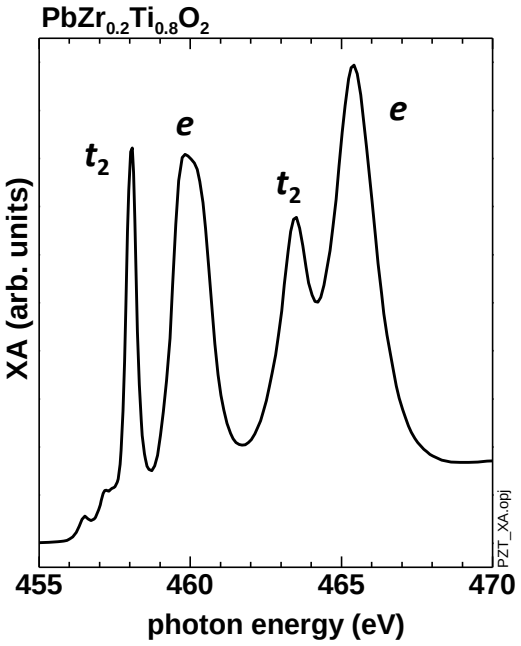

+ Electric dipole transitions: $d^0 \rightarrow 2p^5 3d^1$

+ Crystal field splitting $10Dq$ acting on $3d$ orbitals:

Octahedral symmetry:

e orbitals towards ligands $\rightarrow$ higher energy

t_2 orbitals between ligands $\rightarrow$ lower energy

Tetragonal symmetry:

e orbitals $\rightarrow b_2 = d_{xy}$, $e = d_{yz}, d_{yz}$

t_2 orbitals $\rightarrow b_1 = d_{x^2-y^2}$, $a_1 = d_{3z^2-r^2}$

X-Ray Absorption – Lattice Symmetry

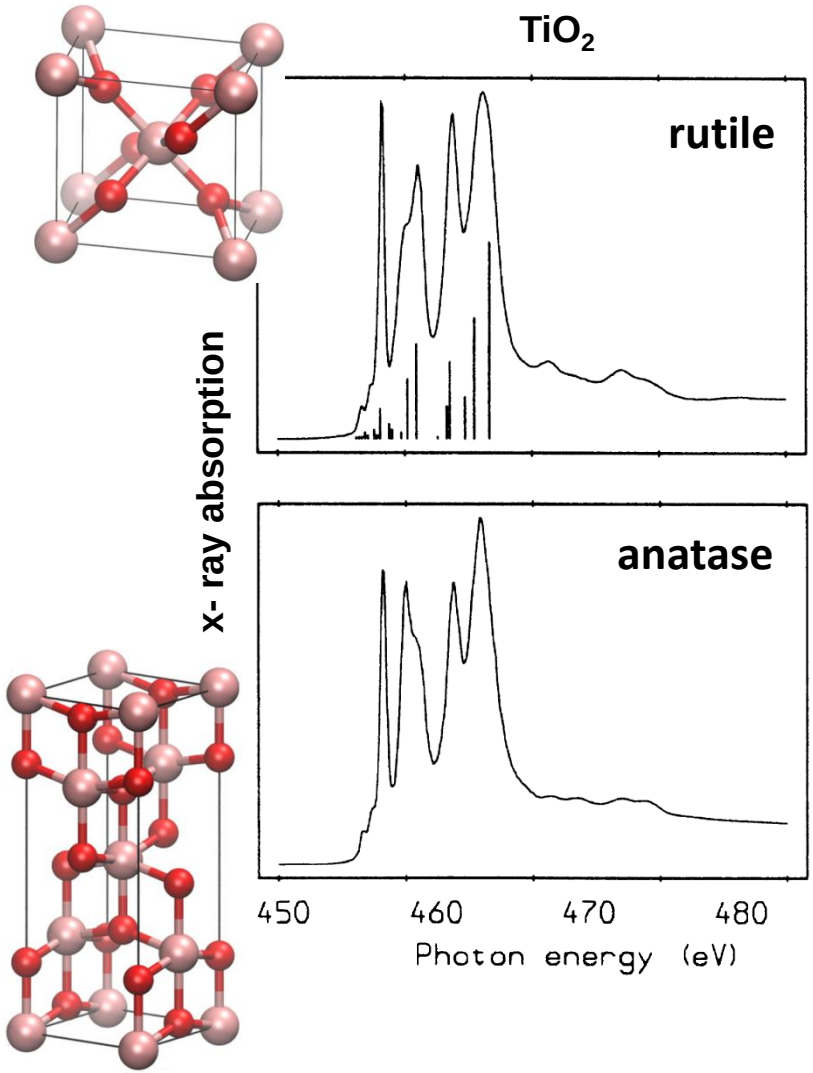

Influence of lattice site symmetry at the absorber

G. Van der Laan
Phys. Rev. B 41, 12366 (1990)

X-Ray Absorption – Fundamentals

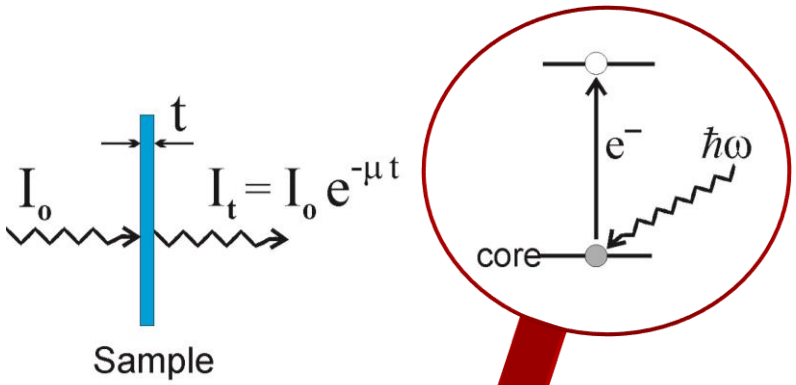

Experimental Concept:

Monitor reduction in x-ray flux transmitted through sample as function of photon energy

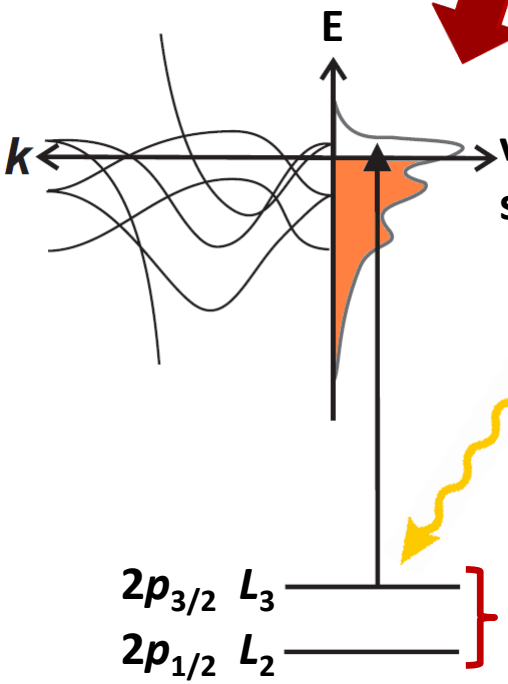

⇒ charge state of absorber Fe^{2+}, Fe^{3+}

⇒ symmetry of lattice site of absorber: O_h, T_d

⇒ sensitive to magnetic order

⇒ Absorption probability: x-ray energy, x-ray polarization, experimental geometry

core level ⇒ atomic species of absorber Fe, Co, Ni, ….

X-Ray Absorption – Fundamentals

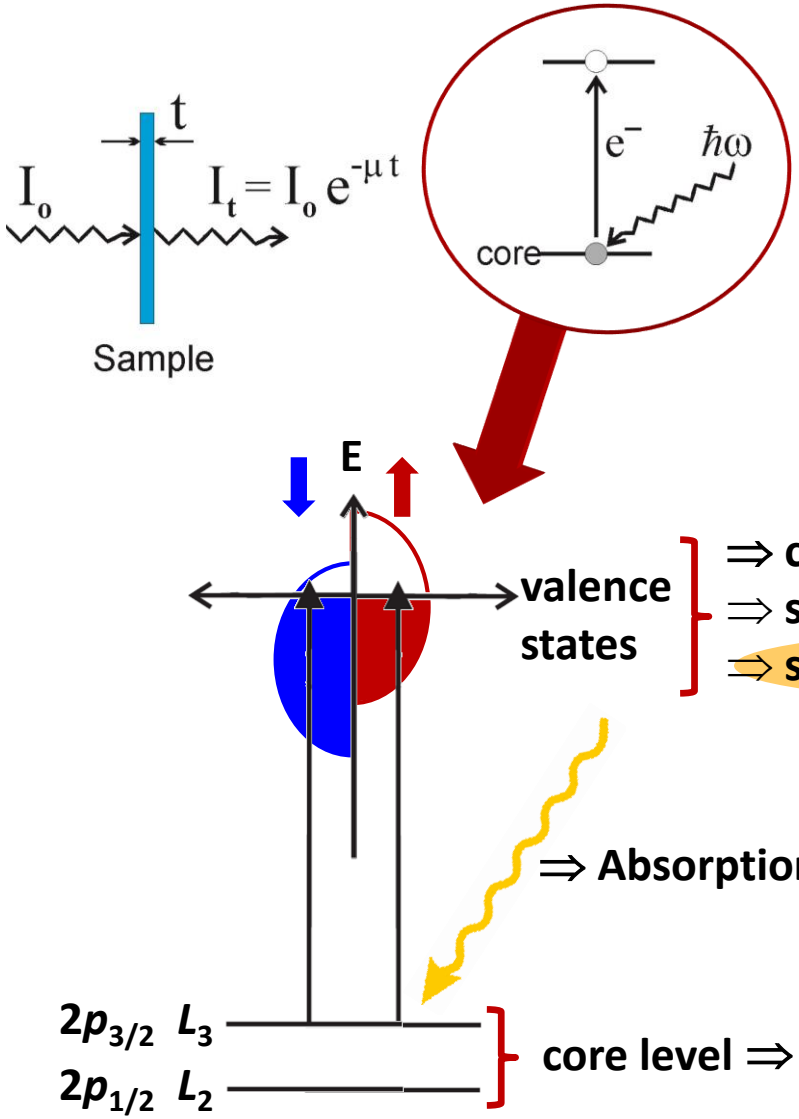

Experimental Concept:

Monitor reduction in x-ray flux transmitted through sample as function of photon energy

⇒ charge state of absorber Fe^{2+}, Fe^{3+}

⇒ symmetry of lattice site of absorber: O_h, T_d

⇒ sensitive to magnetic order

⇒ Absorption probability: x-ray energy, x-ray polarization, experimental geometry

core level ⇒ atomic species of absorber Fe, Co, Ni, ….

Stoner Model For Ferromagnetic Metals

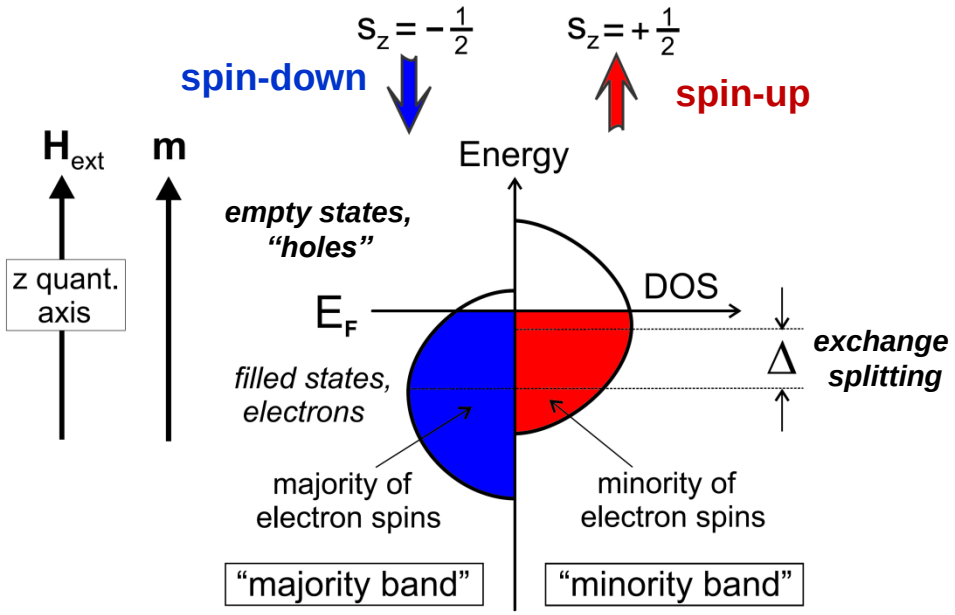

J. Stöhr, H.C. Siegmann, Magnetism (Springer)

3*d* shell

- **Magnetic moments in Fe, Co, Ni well described by Stoner model: *d*-bands containing up and down spins shifted relative to each other by exchange splitting**
- **Spin-up and spin-down bands filled according to Fermi statistics**
- **Magnetic moment |m| determined by difference in number of electrons in majority and minority bands**

$$|m| \propto \mu_B (n_e^{maj} - n_e^{min})$$

Stoner Model For Ferromagnetic Metals

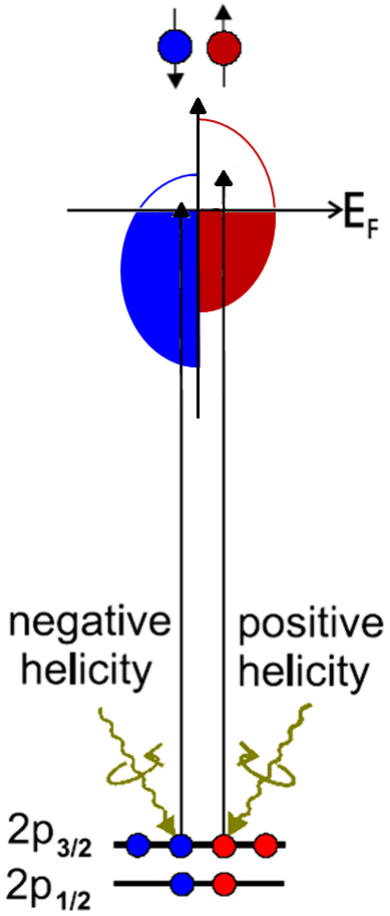

+ Calculate transition probabilities from filled $2p_{3/2}$ and $2p_{1/2}$ states to empty states in *d*-band for circularly polarized x rays using Fermi's golden rule
+ Right/left circularly polarized photons with angular momentum q = +/-1 in units of ħ
+ Important: Spin of the excited electron remains the same

Origin of X-ray Magnetic Circular Dichroism

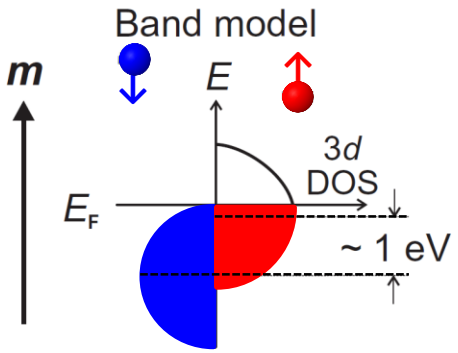

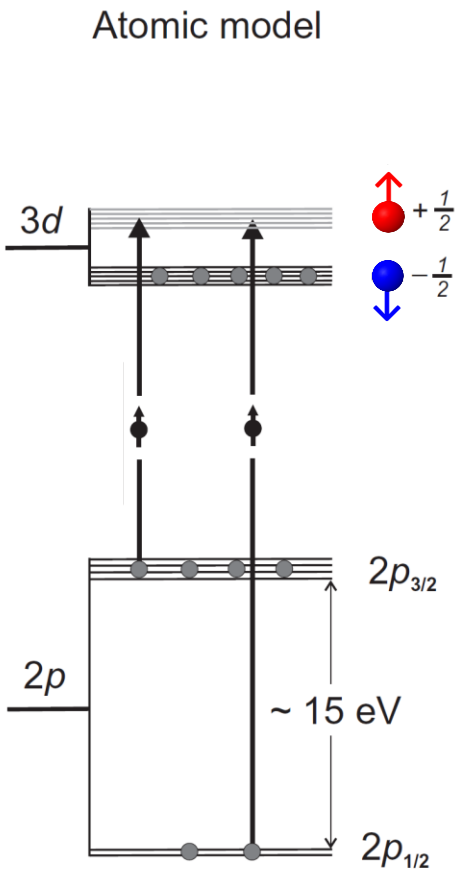

X-ray absorption of circularly polarized photons with angular momentum $q = \pm 1$ in units of ħ

J. Stöhr, H.C. Siegmann, Magnetism (Springer)

+ **Consider strong ferromagnet with one filled spin band:**
  - **All spin down *d* states filled**
  - **Spin up *d* states partially filled**

+ **This specific case: Only spin up electron excited**

ORIGIN OF X-RAY MAGNETIC CIRCULAR DICHROISM

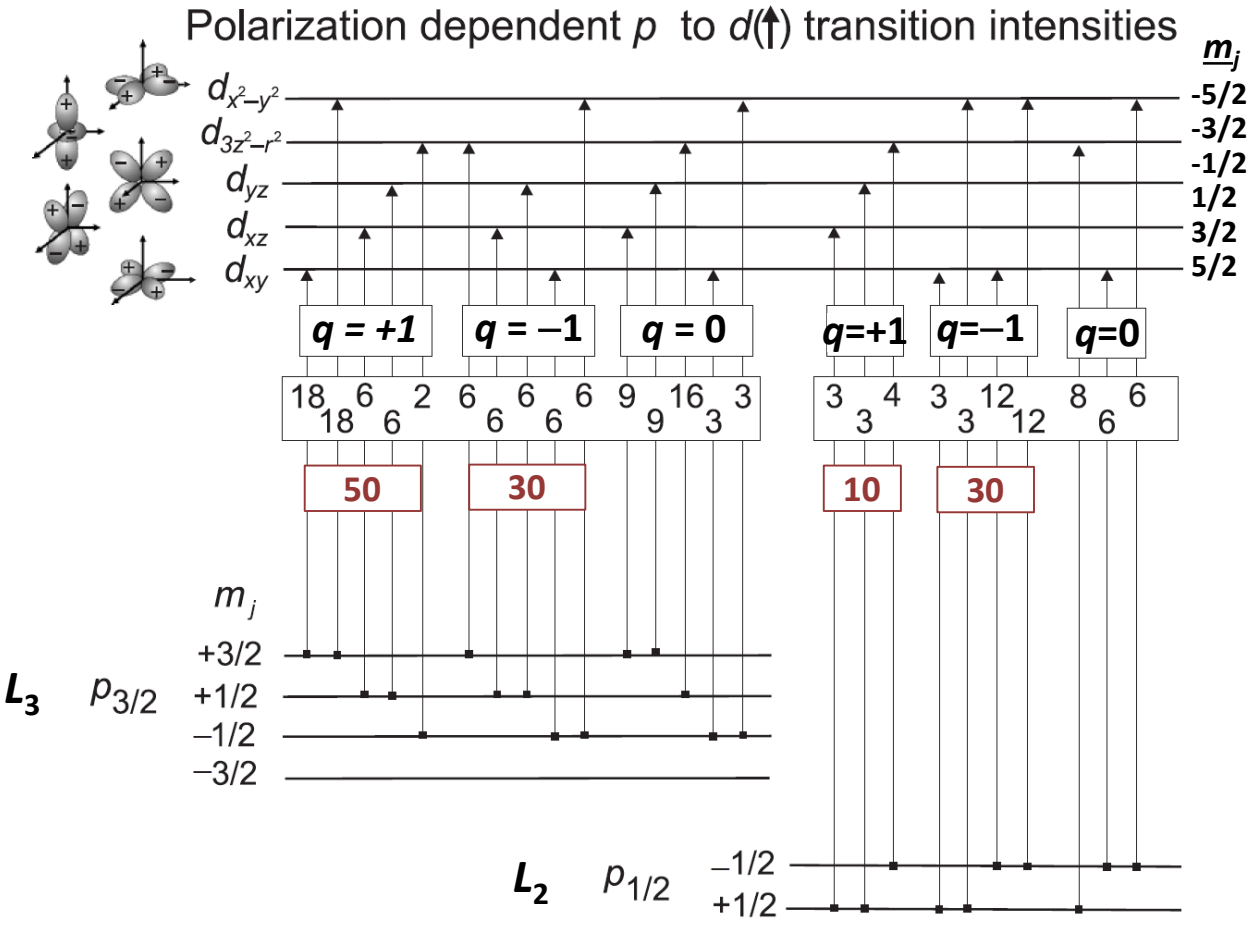

J. Stöhr, H.C. Siegmann, Magnetism (Springer)

L_3: X rays with q = +/–1 excite 62.5%/37.5% of the spin up electrons

L_2: X rays with q = +/–1 excite 25%/75% of the spin up electrons

Origin of X-ray Magnetic Circular Dichroism

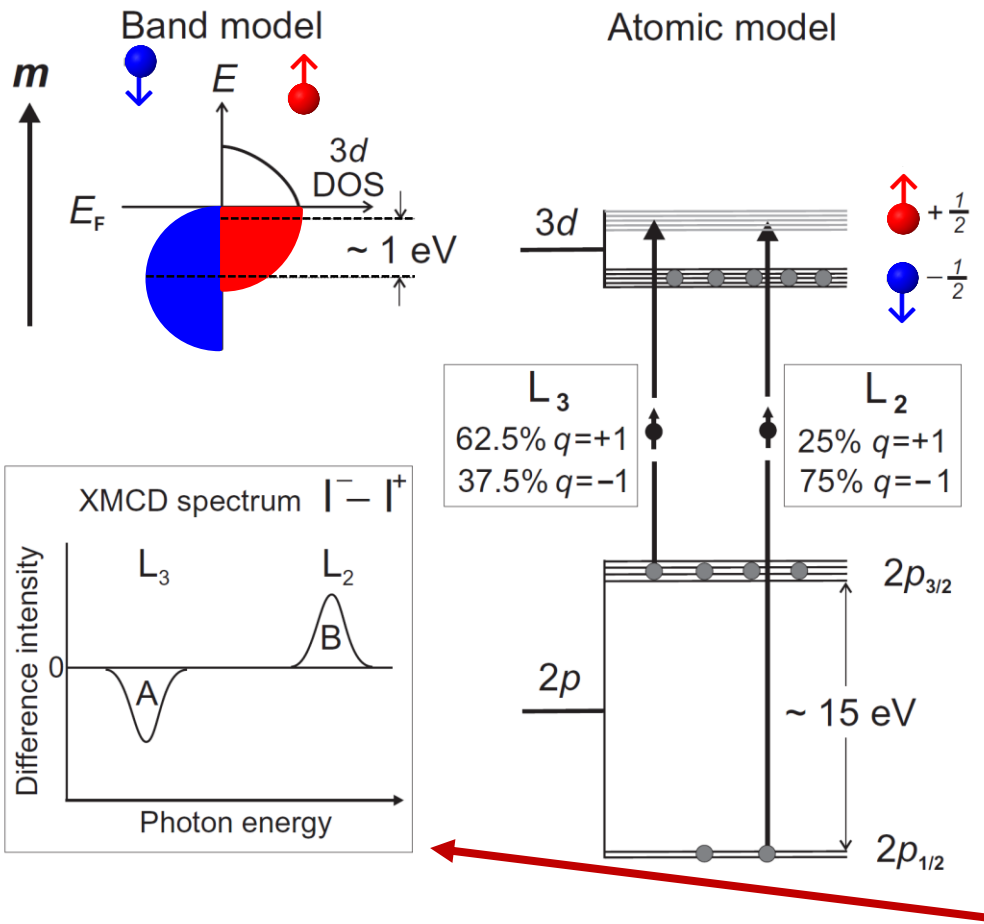

L_3: X rays with q = +1 excite 62.5% spin up electrons
X rays with q = – 1 excite 37.5% spin up electrons
Δ = 25%

L_2: : X rays with q = +1 excite 25% spin up electrons
X rays with q = – 1 excite 75% spin up electrons
Δ = 50%

Taking into account 2x higher population of $2p_{3/2}$ state as compared to $2p_{1/2}$ state:

$\Rightarrow$ Identical magnitude XMCD at L_3 and L_2 with opposite sign

Contributions of $p \rightarrow d$ transitions dominate $p \rightarrow s$ transitions by factor >20.

X-Ray Magnetic Circular Dichroism (XMCD)

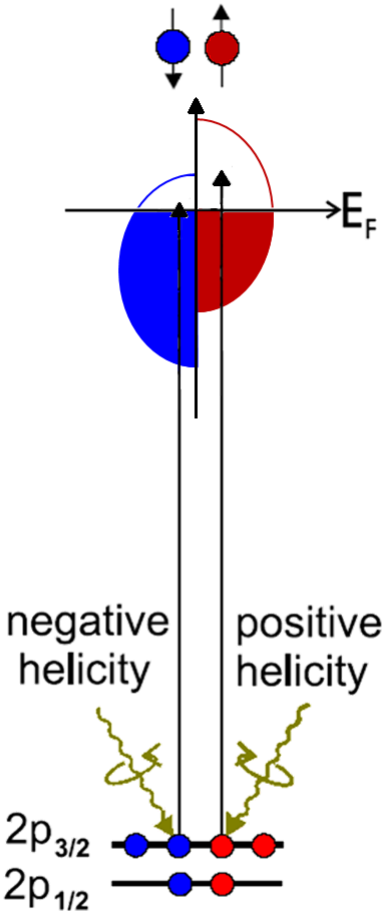

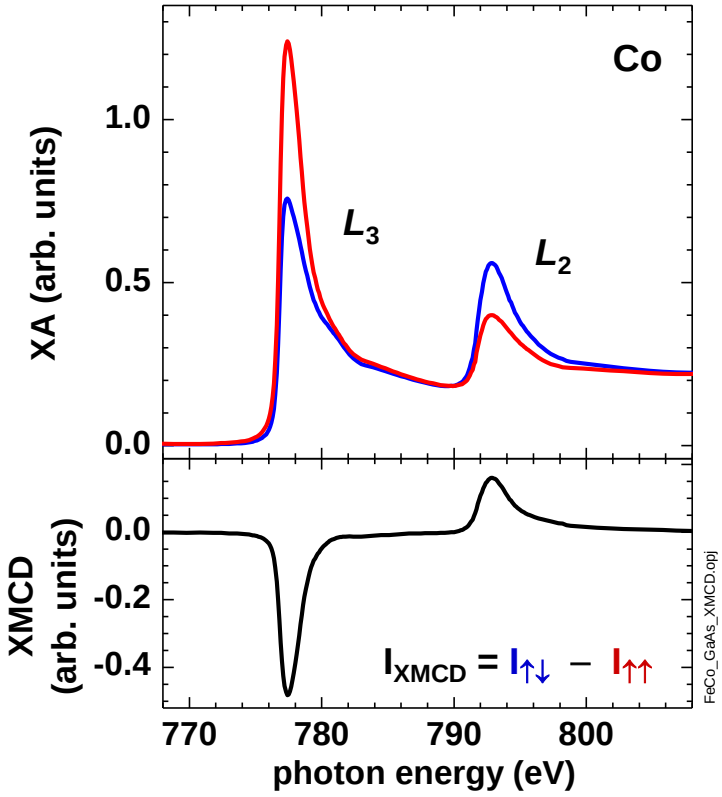

Magnitude of XMCD depends on

- **+ expectation value of 3*d* magnetic moment**
- **+ degree of circular photon polarization, P_{circ}**
- **+ geometry**

X-Ray Magnetic Circular Dichroism (XMCD)

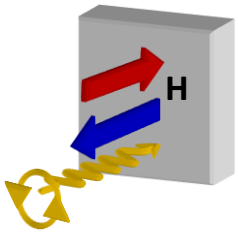

circularly polarized

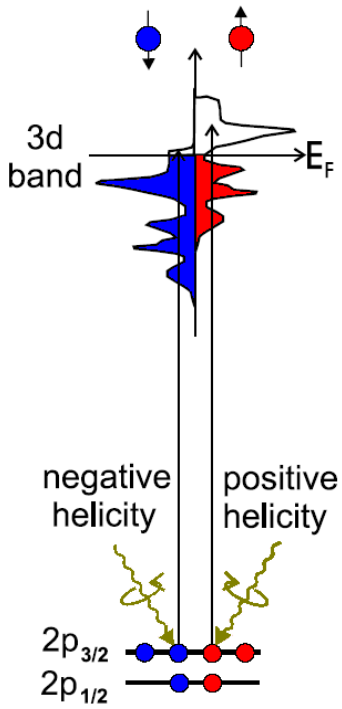

J. Stöhr, H.C. Siegmann, Magnetism (Springer)

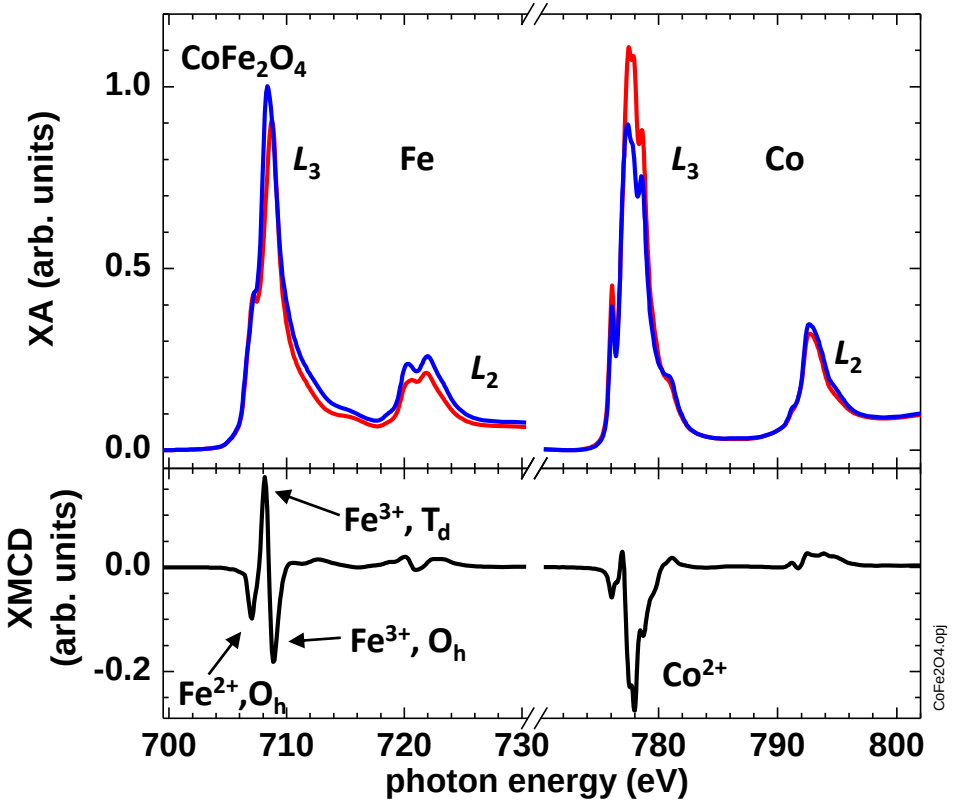

+ XMCD provides magnetic information resolving elements Fe, Co, …
valence states: Fe^{2+}, Fe^{3+}, …
lattice sites: octahedral, O_h, tetrahedral, T_d,

MAGNETIC BIONANOSPINELS

+ Geobacter sulfurreducens bacteria form magnetite nanocrystals (15nm) via extracellular reduction of amorphous Fe(III)-bearing minerals

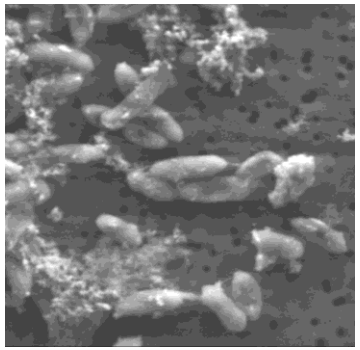

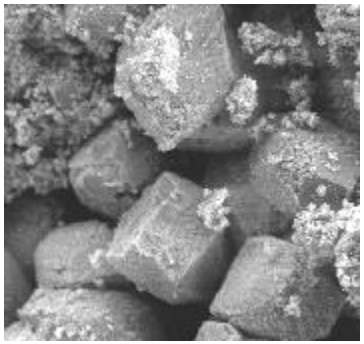

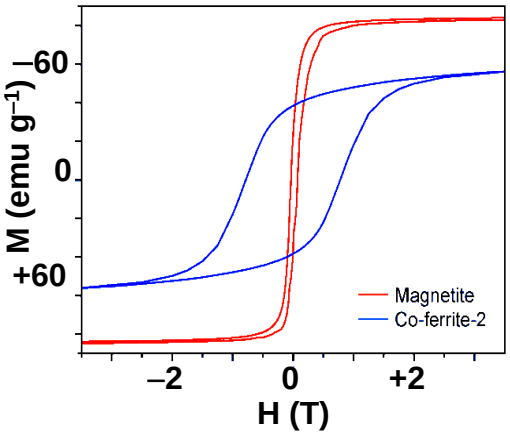

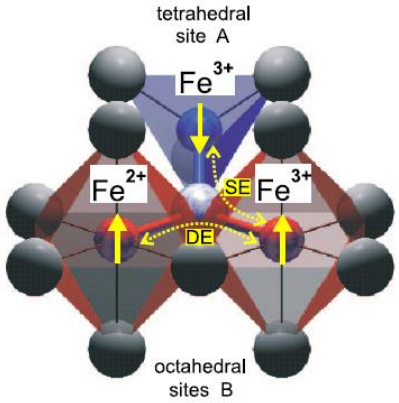

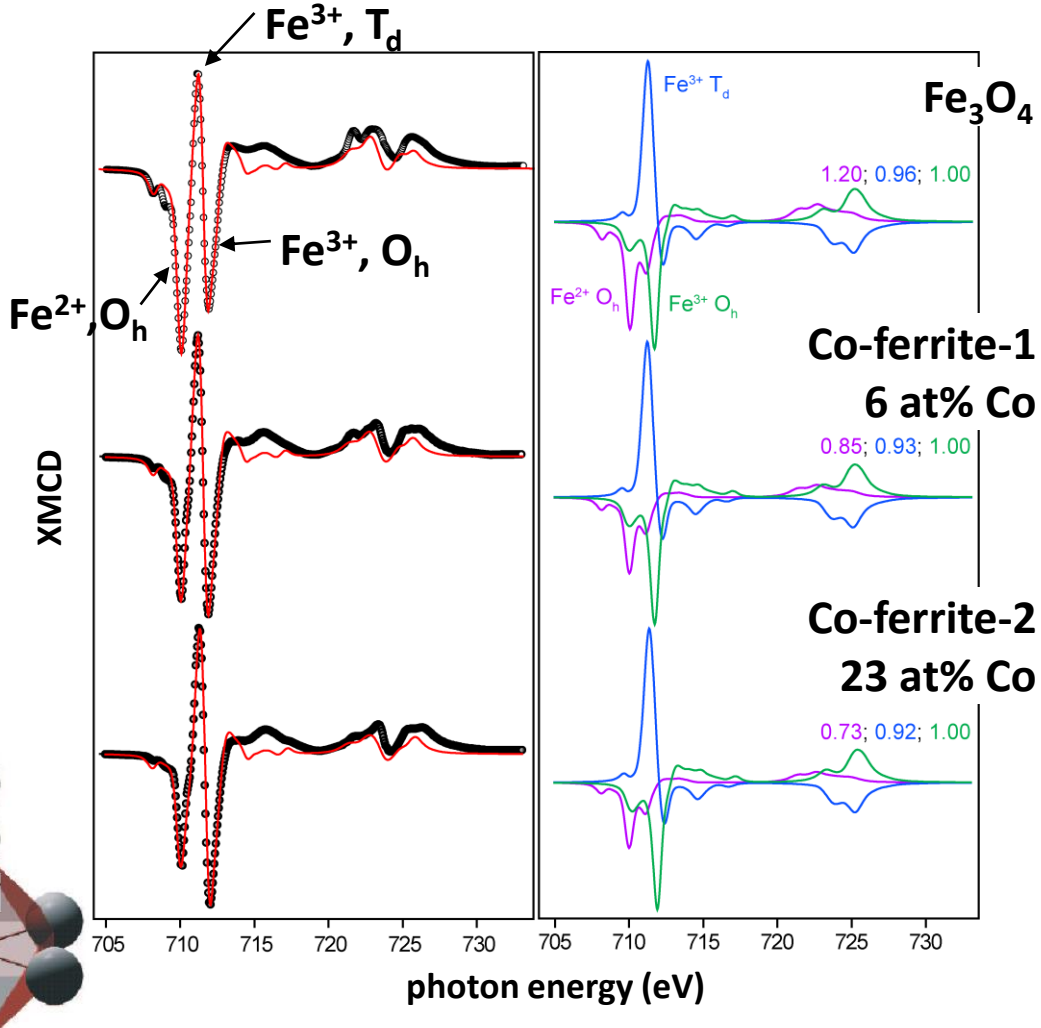

V. Cocker *et al.*,
Eur. J. Mineral. 19, 707–716 (2007)

MAGNETIC BIONANOSPINELS

+ **Geobacter sulfurreducens bacteria form magnetite nanocrystals (15nm) via extracellular reduction of amorphous Fe(III)-bearing minerals**

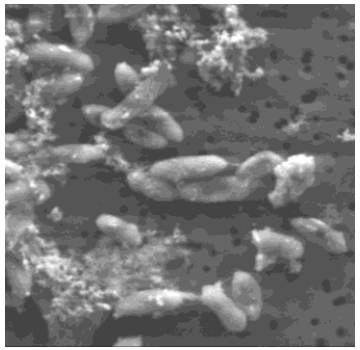

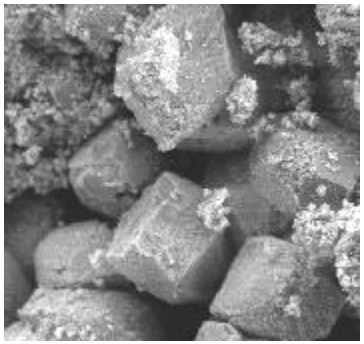

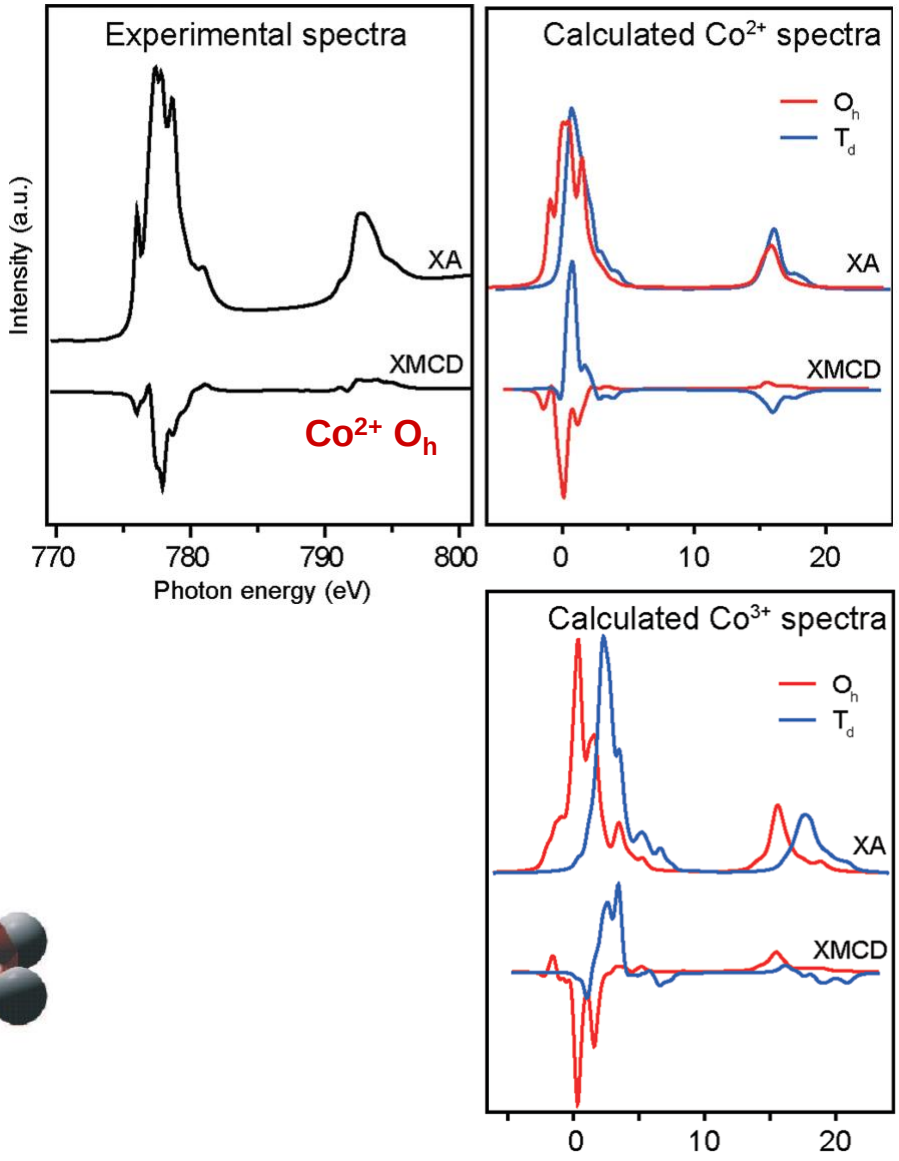

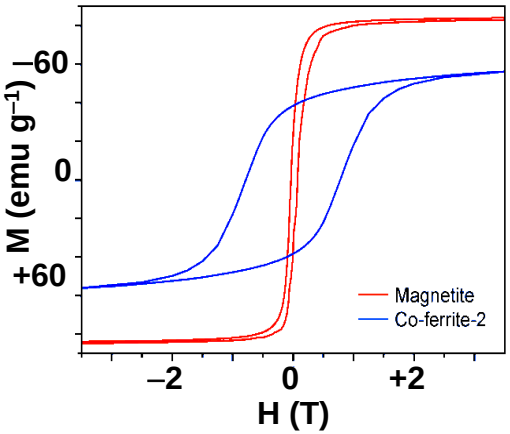

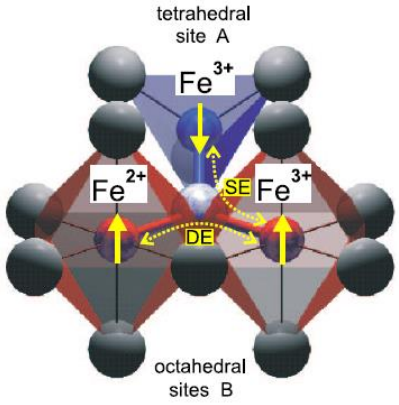

Co-DOPED TiO_2

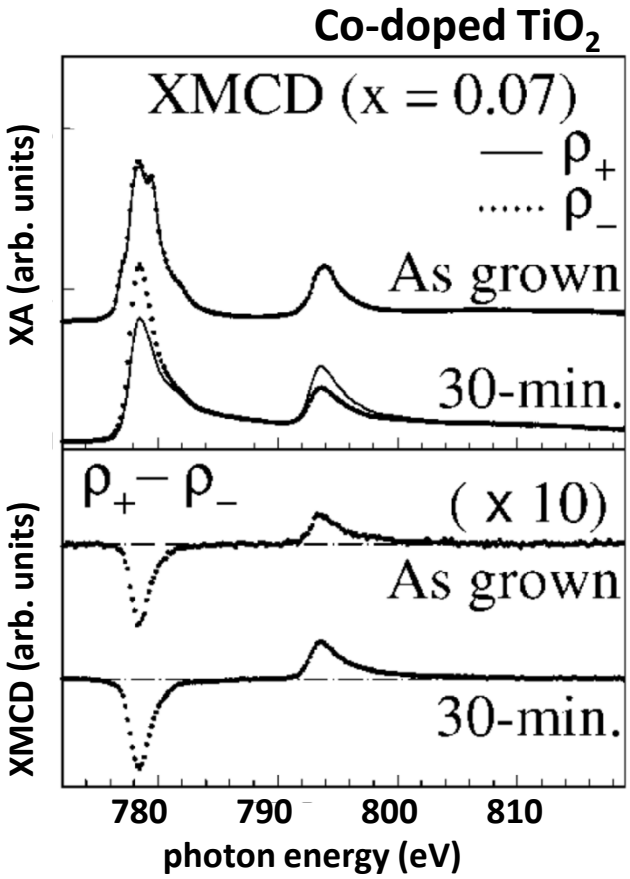

J.-Y. Kim *et al.*,
Phys. Rev. Lett. 90, 017401 (2003)

dilute magnetic semiconductors

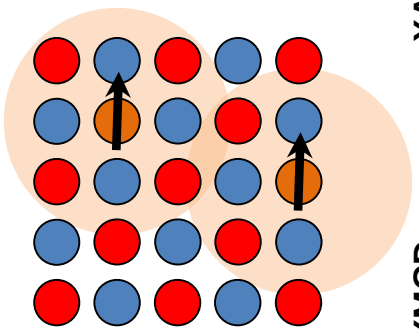

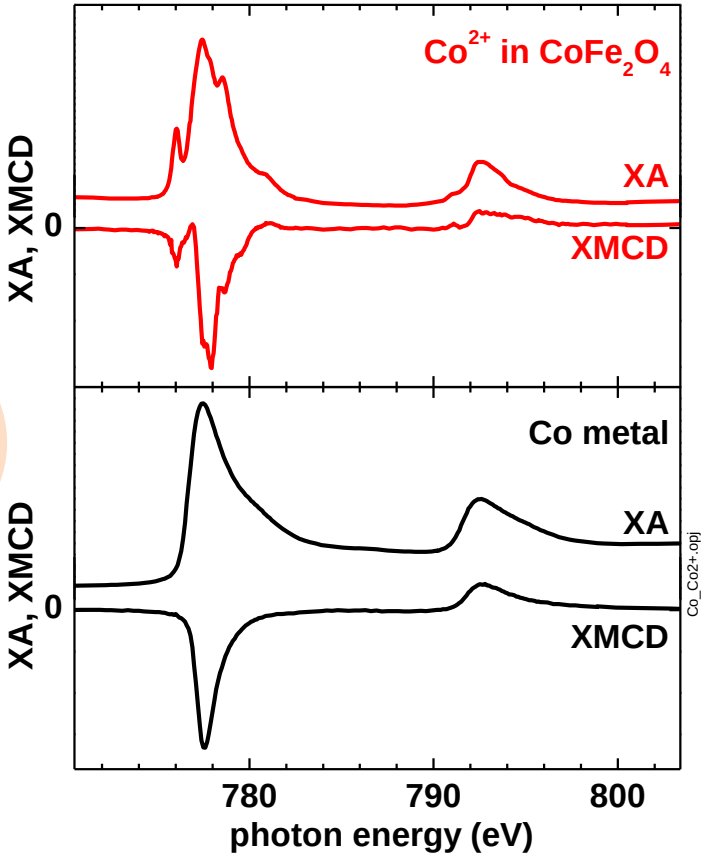

+ Comparing XMCD spectra with model compounds and/or calculations

⇒ Identifying magnetic phases

Induced Moments At Co/Cu Interfaces

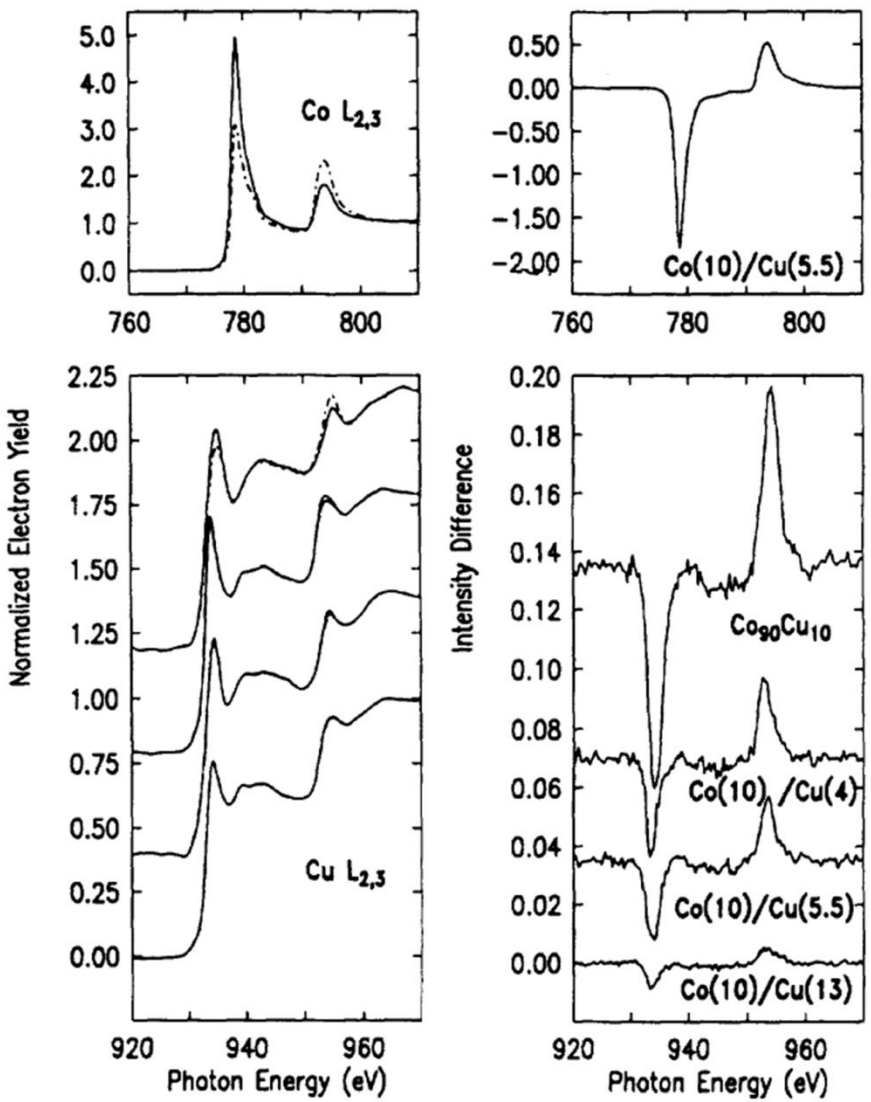

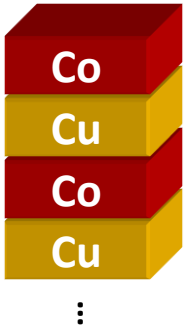

+ **The element-specificity makes XMCD measurements an ideal tool to determine induced moments at interfaces between magnetic and non-magnetic elements.**

M. G. Samant *et al.*,
Phys. Rev. Lett. 72, 1112 (1994)

MAGNETIC INTERFACES

+ Weak Mn XMCD signal

⇒ Uncompensated Mn at Co/IrMn interface

+ Same sign of XMCD signal for Co and Mn

⇒ Parallel coupling of Co and Mn moments

+ Nominal thickness of uncompensated interface moments: (0.5±0.1)ML

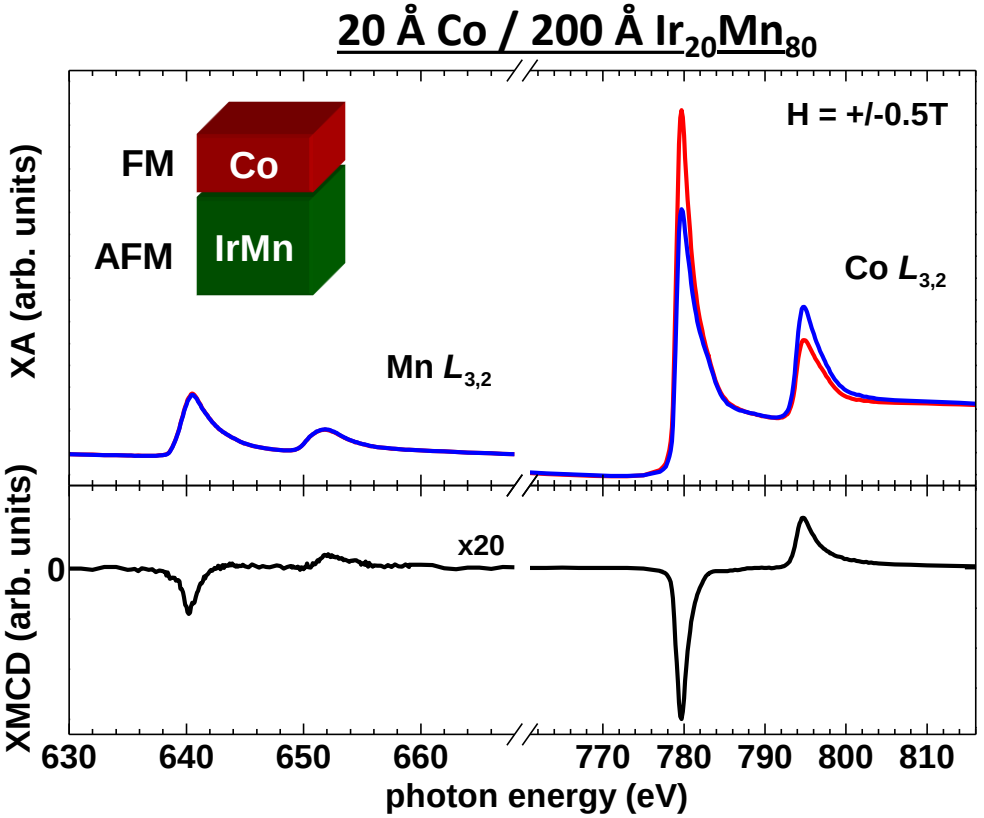

H. Ohldag *et al.*,
Phys. Rev. Lett. 91, 017203 (2003)

Sum Rules

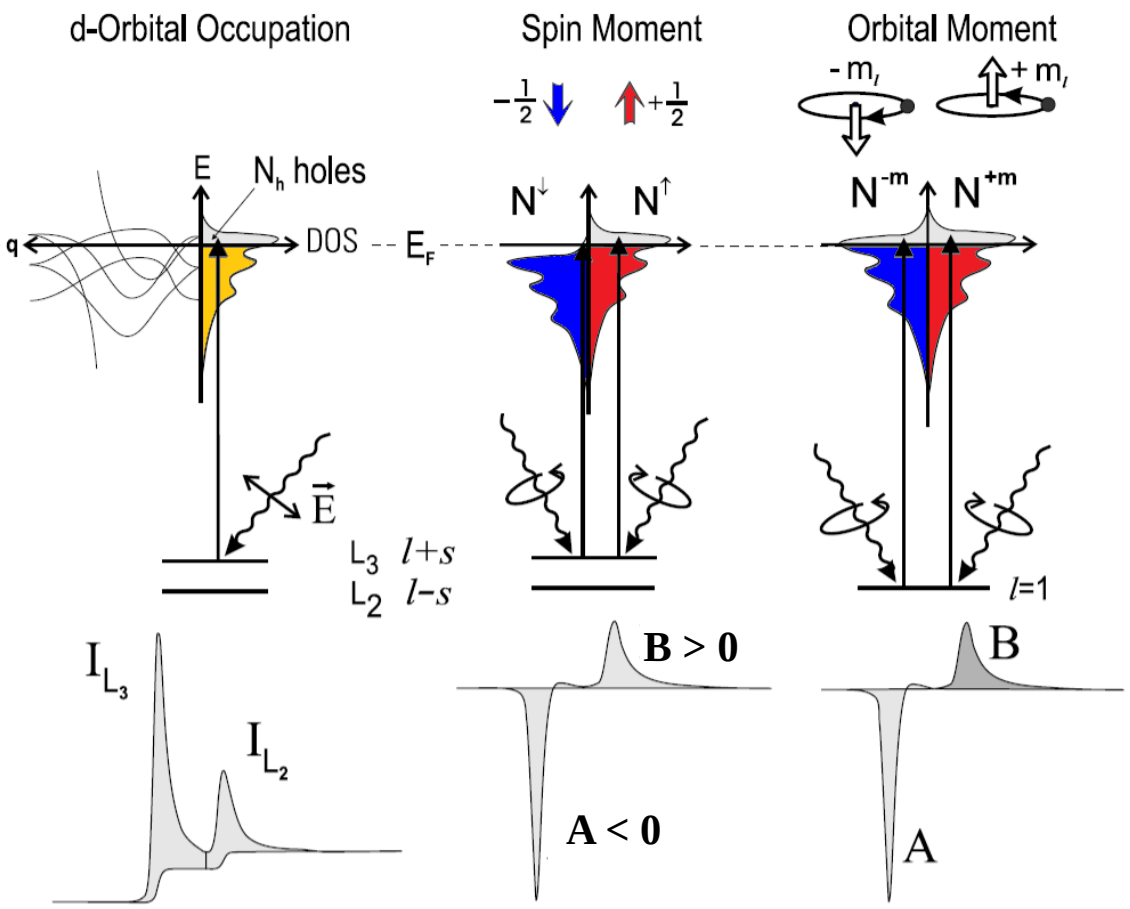

$N_h = \langle I_{L3} + I_{L2} \rangle / C$

$m_S = \mu_B \langle -A + 2B \rangle / C$

$m_L = -2\mu_B \langle A + B \rangle / 3C$

+ **Theoretically derived sum rules correlate XMCD spectra with spin and orbital moment providing unique tool for studying magnetic materials.**

J. Stöhr, H.C. Siegmann, Magnetism (Springer)

Orbital Moment Of Co Nanoparticles

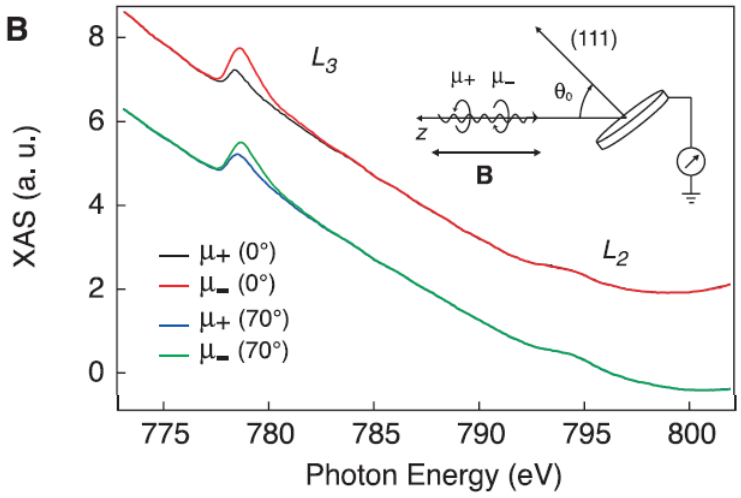

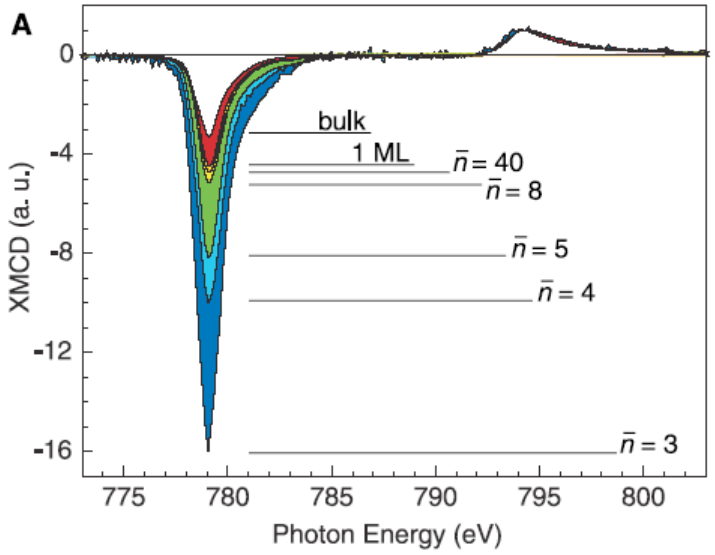

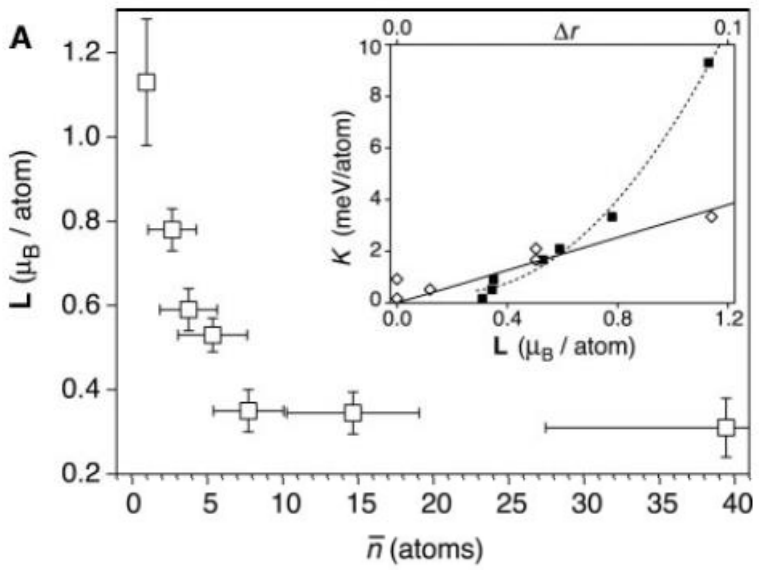

+ **Strong variation of orbital and spin magnetic moment observable as change in relative L_3 and L_2 intensity in XMCD spectrum.**
+ **Co atoms and nanoparticles on Pt have enhanced orbital moments up to 1.1 μ_B**

P. Gambardella *et al.*,
Science 300, 1130 (2003)

ELEMENT-SPECIFIC MAGNETIZATION REVERSAL

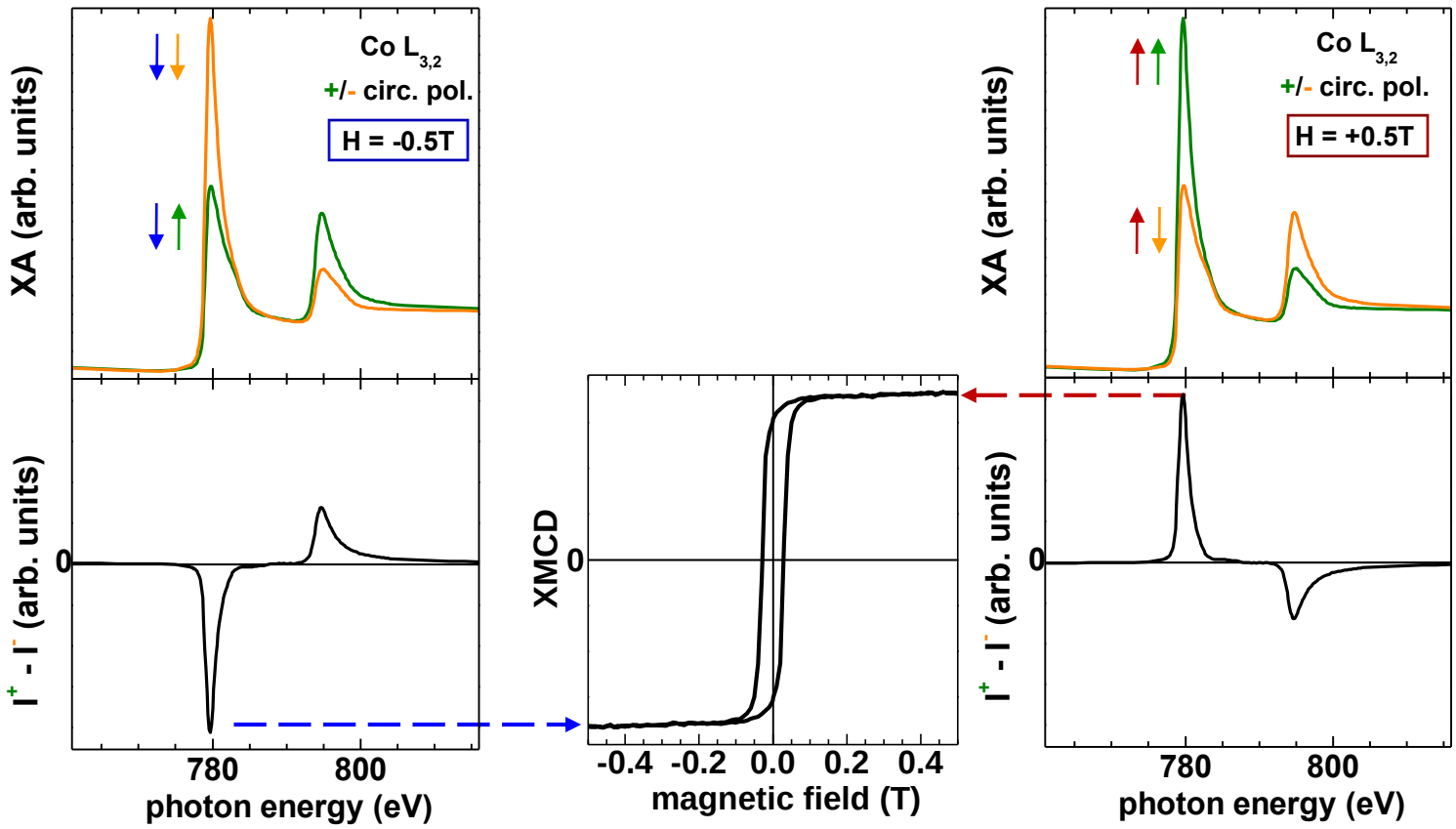

+ **Monitoring field dependence of XMCD**

⇒ **Element-specific information on magnetization reversal in complex magnetic nanostructures.**

Element-specific Magnetization Reversal

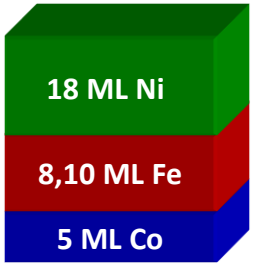

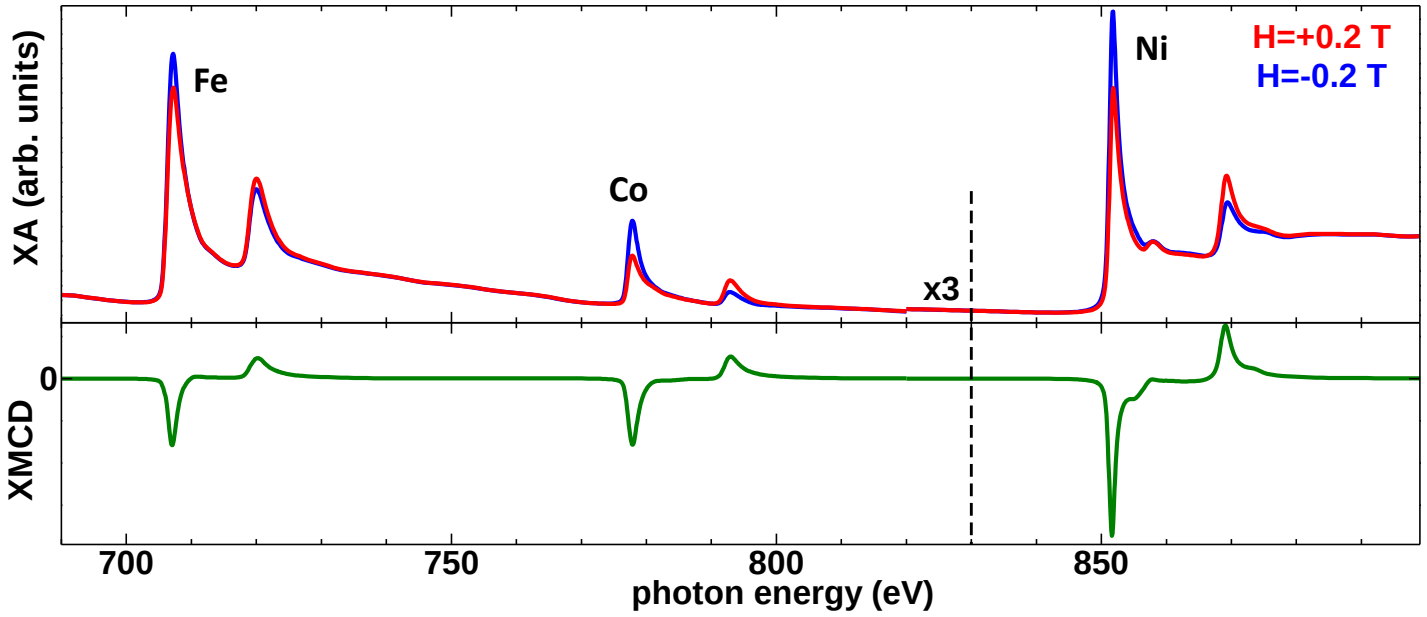

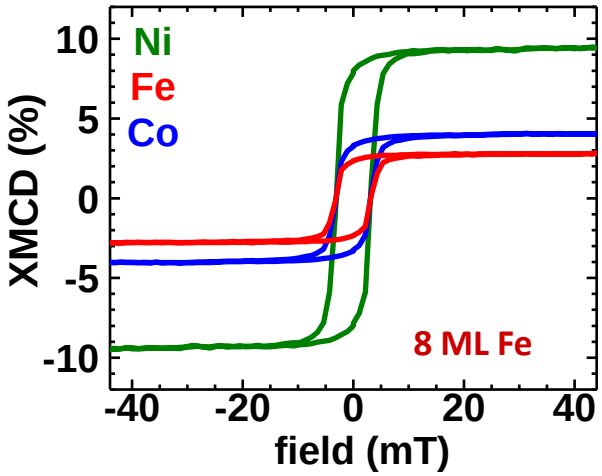

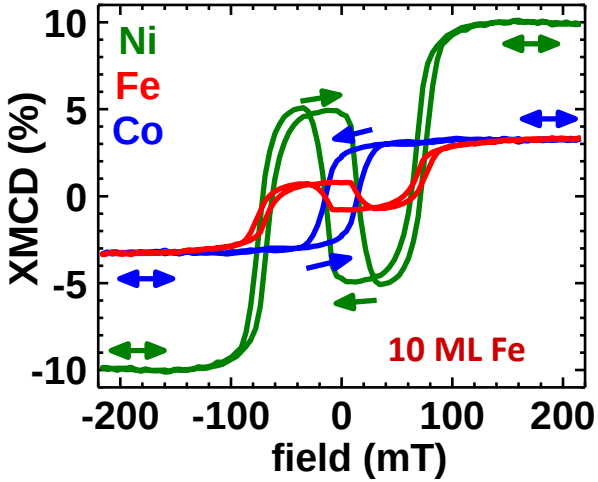

X-Ray Ferromagnetic Resonance

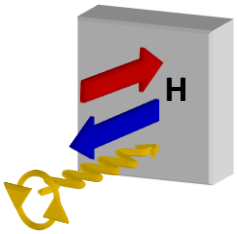

circularly polarized

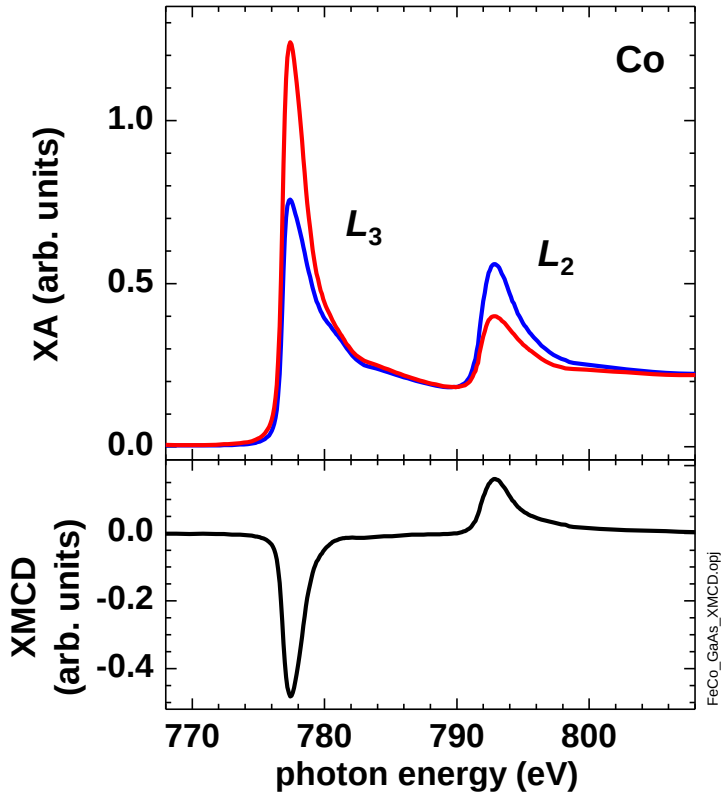

- XMCD is the difference in x-ray absorption between antiparallel and parallel orientation of magnetic moment and photon spin.
- The XMCD magnitude reflects the magnetic moment aligned parallel to the x ray beam.

X-Ray Ferromagnetic Resonance

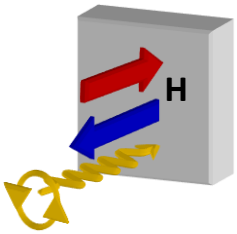

circularly polarized

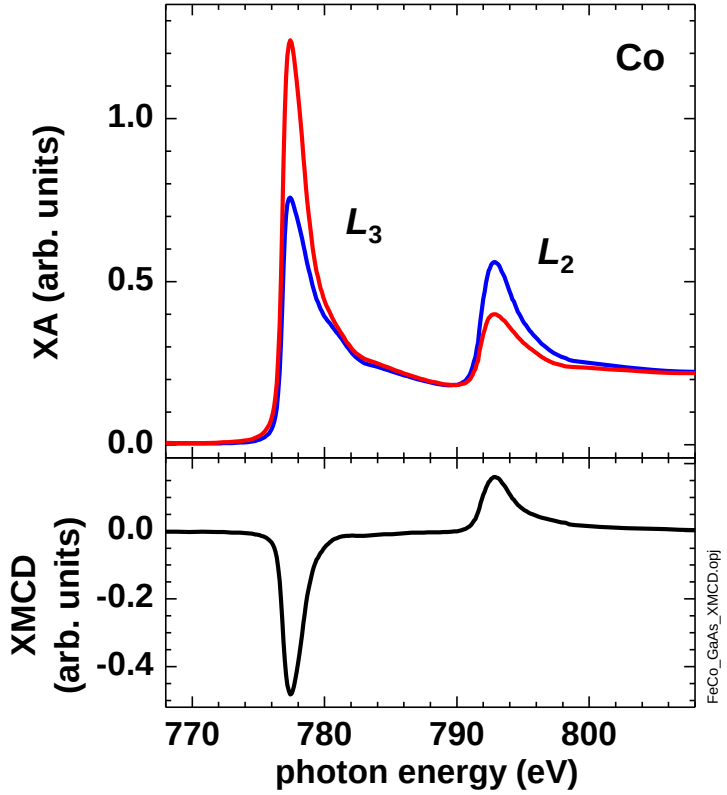

+ **In fact:**
  Magnetic moments are not fully aligned with applied fields but precess around them.

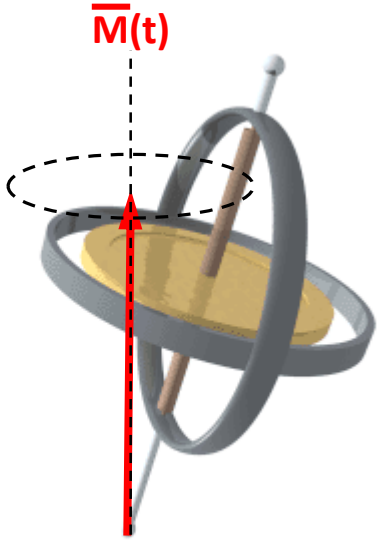

X-Ray Ferromagnetic Resonance

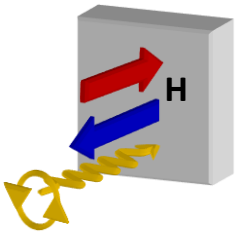

circularly polarized

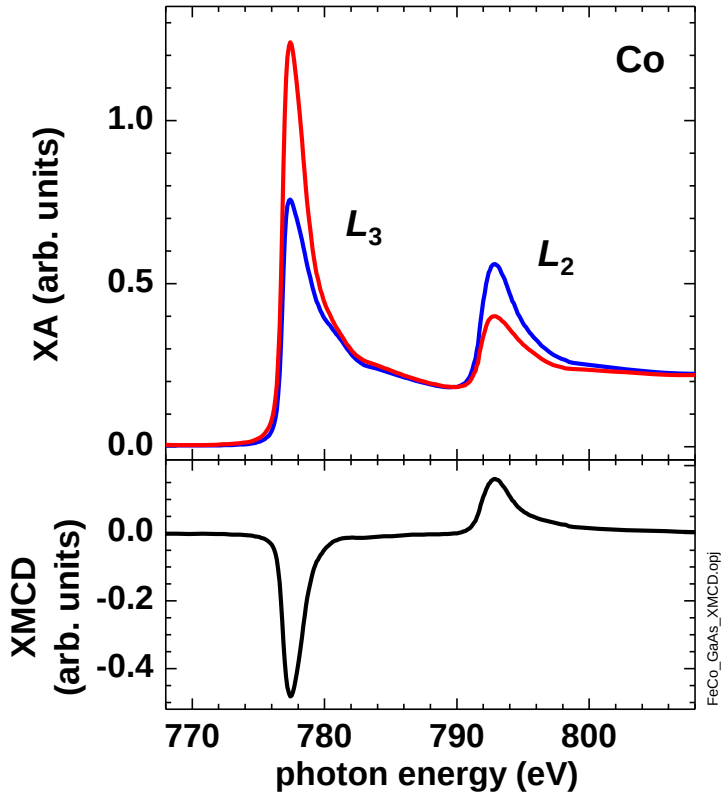

+ **In fact:**
  Magnetic moments are not fully aligned with applied fields but precess around them.

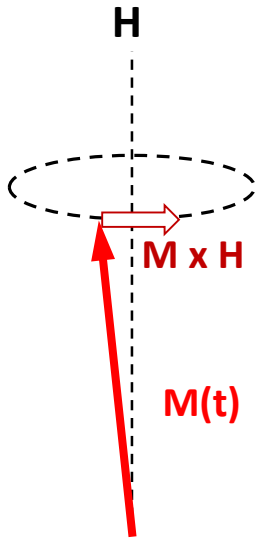

+ **Is it possible to measure the pression of magnetic moments making use of the pulsed nature of synchrotron radiation and XMCD?**

X-Ray Ferromagnetic Resonance

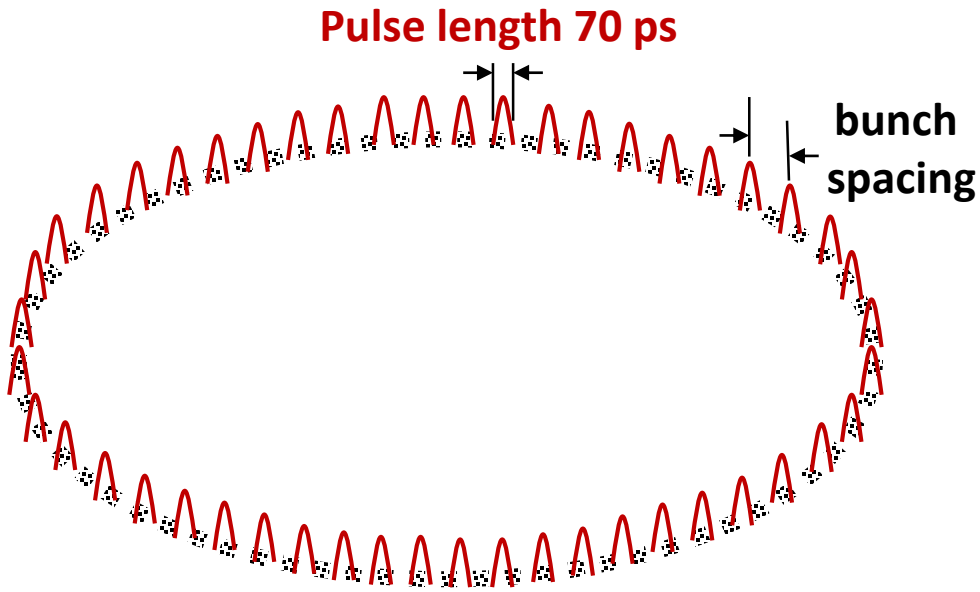

Pulsed nature of synchrotron radiation
Example: Advanced Light Source

- 256-320 bunches for 500mA beam current
- Bunch spacing: 2 ns
- Pulse length 70ps

X-Ray Ferromagnetic Resonance

Dynamic XMCD measurement, i.e. synchronize x-ray pulses with FMR precession

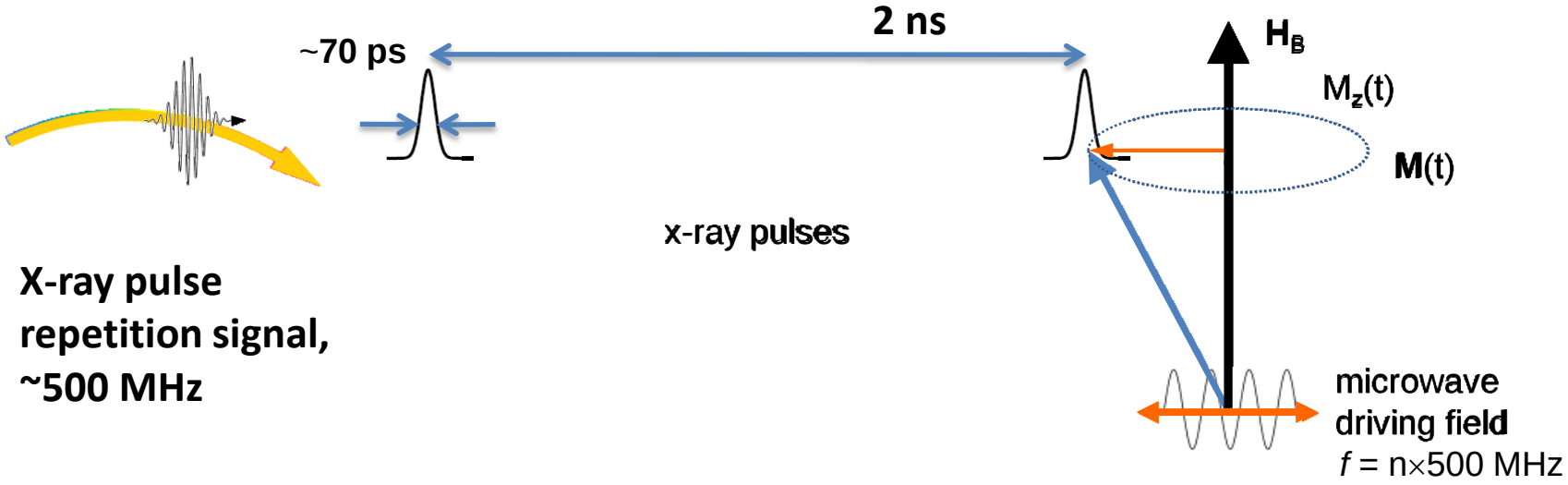

X-ray pulse repetition signal, ~500 MHz

X-RAY FERROMAGNETIC RESONANCE

Static XMCD

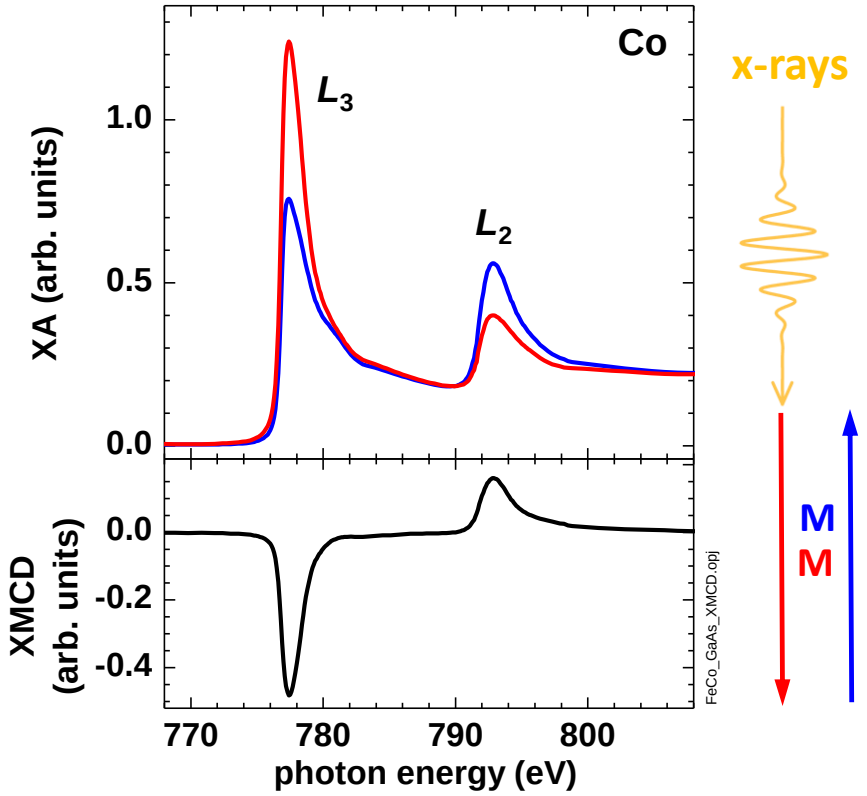

Dynamic XMCD

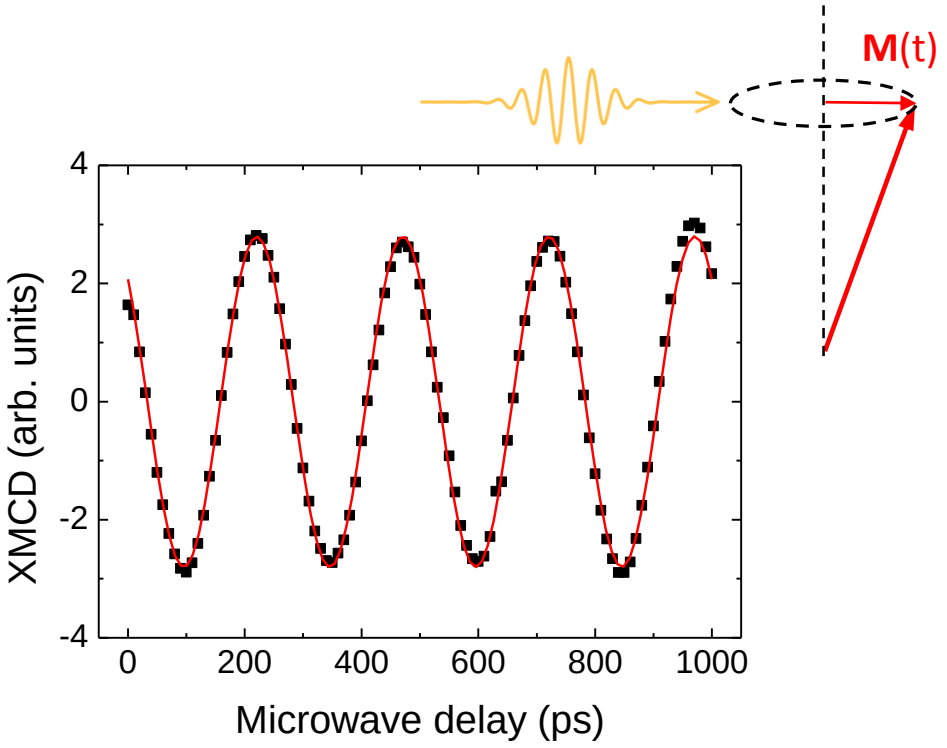

X-Ray Ferromagnetic Resonance

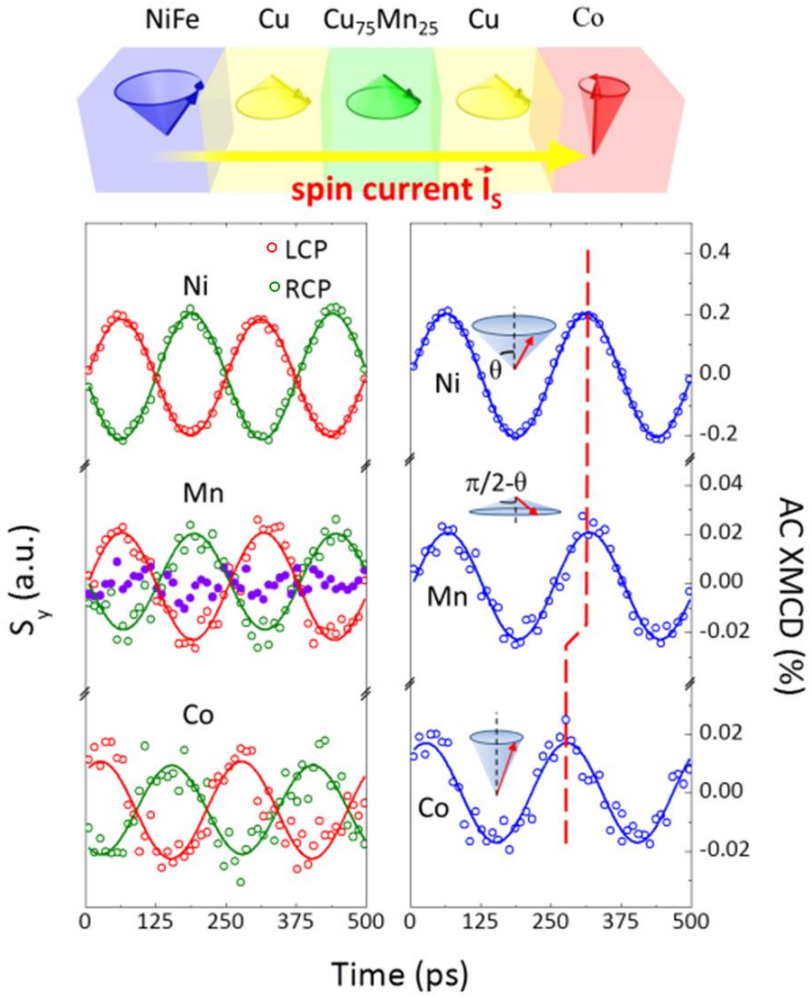

+ Precession is resonantly excited in the NiFe layer with an 4 GHz RF field.
+ The resonance field of the CO layer is higher, i.e. no precession is excited in the Co layer.
+ Precession in Py, $Cu_{75}Mn_{25}$, and Co layers are probed by XMCD using left- and right-circularly polarized x-rays at Ni, Mn, and Co edges, respectively.
+ The $Cu_{75}Mn_{25}$ spin precession is a direct indicator of the AC spin current through the structure.

X-Ray Linear Dichroism

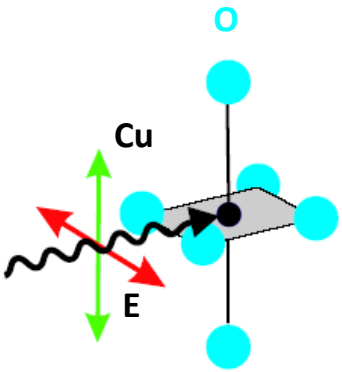

C. T. Chen *et al.*
PRL 68, 2543 (1992)

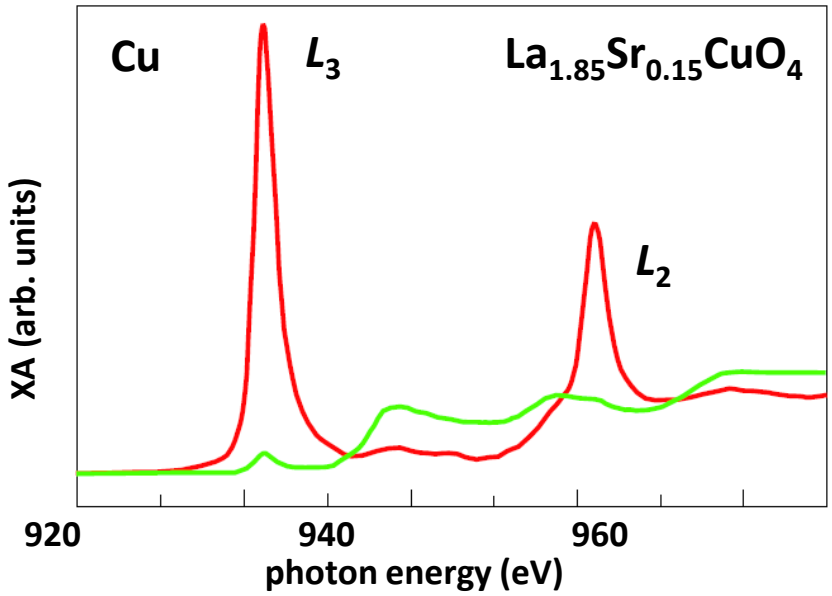

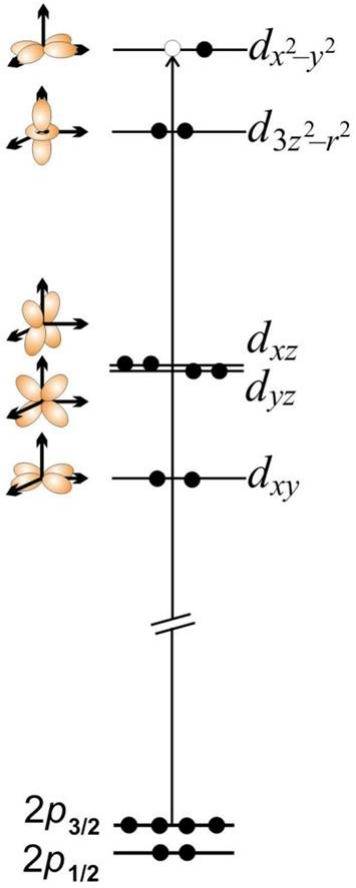

X-Ray Linear Dichroism:

+ Difference in x-ray absorption for different linear polarization direction relative to crystalline and/or spin axis.
+ Due to the anisotropic charge distribution about the absorbing atom caused by bonding and/or magnetic order.
+ "Search Light Effect": X-ray absorption of linear polarized x rays proportional to density of empty valence states in direction of electric field vector E.

Structural Changes In $PbZr_{0.2}Ti_{0.8}O_3$

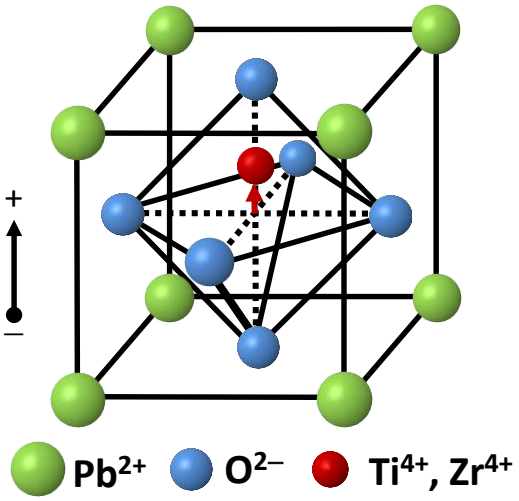

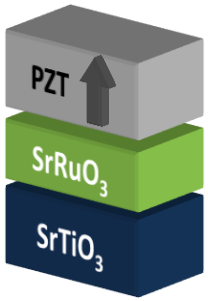

ferroelectric polarization

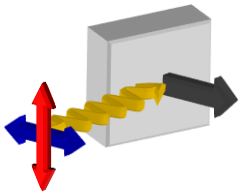

as grown

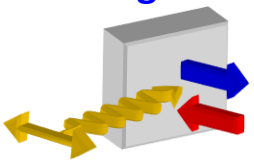

reversed

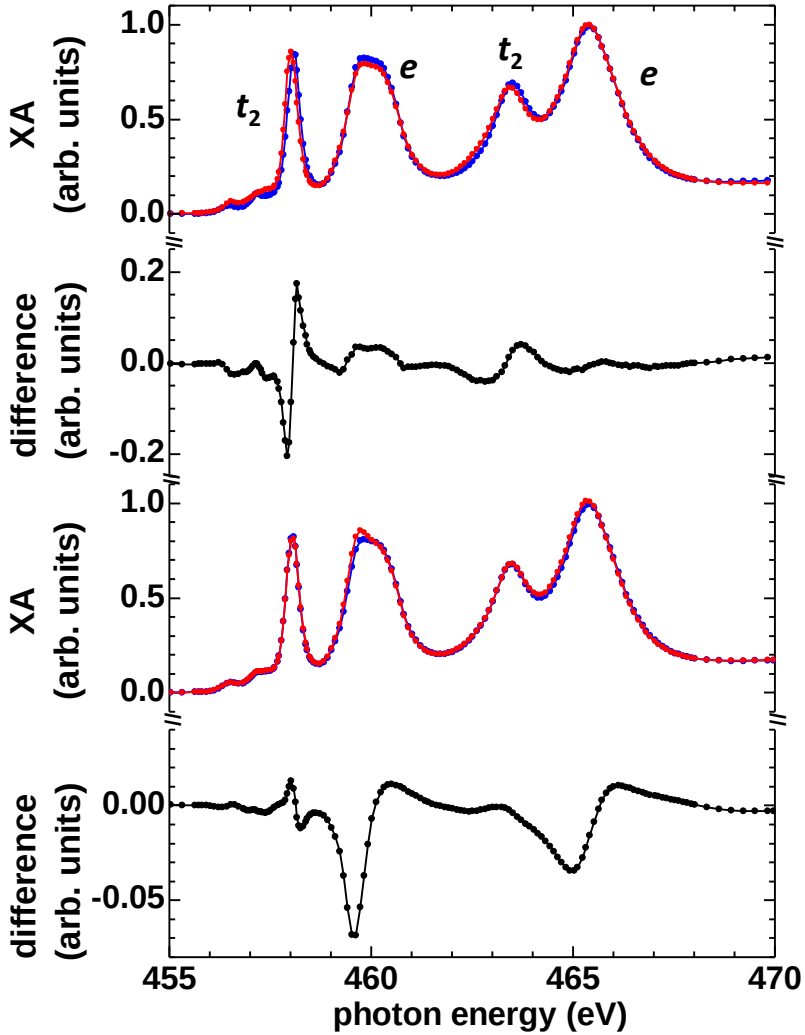

E. Arenholz *et al.*,
Phys. Rev. B 82, 140103 (2010)

+ Spontaneous electric polarization due to off-center shift of Ti^{4+}, Zr^{4+} associated with tetragonal distortion ⇔ linear dichroism

+ Reversing ferroelectric polarization changes XA ⇔ Change in tetragonal distortion

X-Ray Magnetic Linear Dichroism

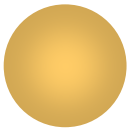

Isotropic *d* electron charge density
⇒ No polarization dependence

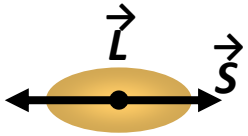

Magnetically aligned system
⇒ Spin-orbit coupling distorts charge density
⇒ Polarization dependence

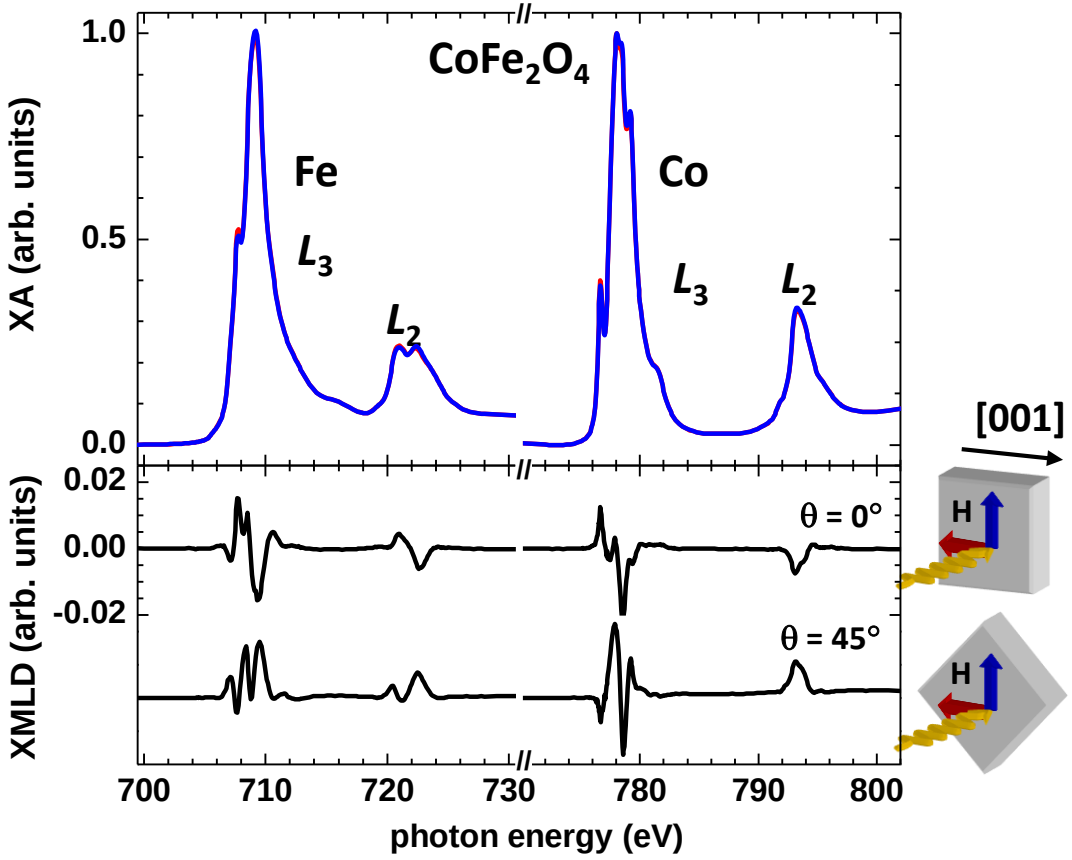

+ $I_{XMLD} = I_{||} - I_{\perp} \propto \langle m^2 \rangle$, $\langle m^2 \rangle$ = expectation value of square of atomic magnetic moment
+ XMLD allows investigating ferri- and ferromagnets as well as antiferromagnets
+ XMLD spectral shape and angular dependence are determined by magnetic order and lattice symmetry

X-Ray Magnetic Linear Dichroism

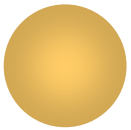

Isotropic *d* electron charge density
⇒ No polarization dependence

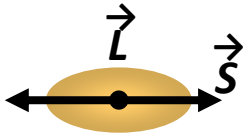

Magnetically aligned system
⇒ Spin-orbit coupling distorts charge density
⇒ Polarization dependence

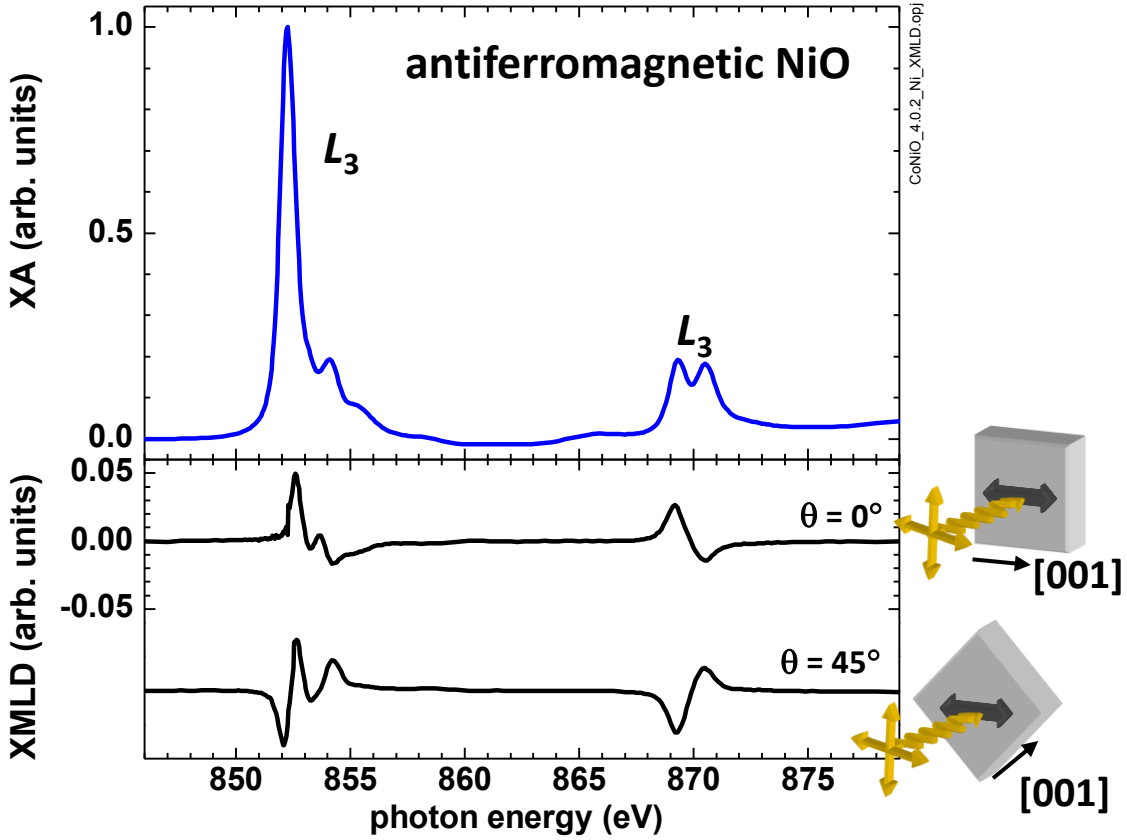

+ $I_{XMLD} = I_{||} - I_{\perp} \propto \langle m^2 \rangle$, $\langle m^2 \rangle$ = expectation value of square of atomic magnetic moment
+ XMLD allows investigating ferri- and ferromagnets as well as antiferromagnets
+ XMLD spectral shape and angular dependence are determined by magnetic order and lattice symmetry

Magnetic Coupling At Interfaces

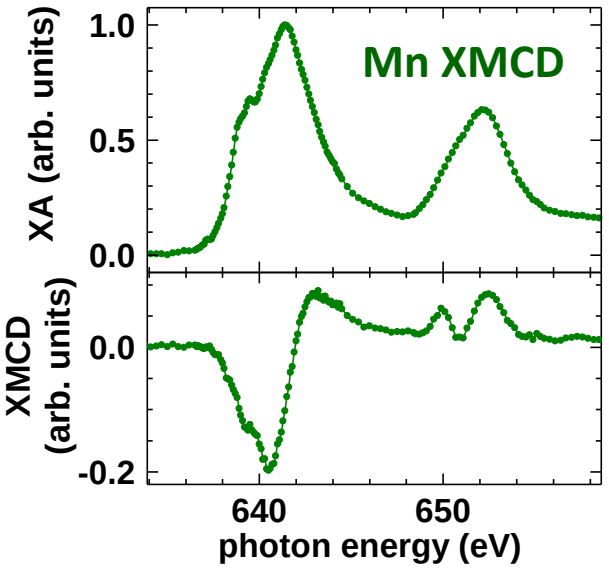

$La_{0.7}Sr_{0.3}MnO_3$ (LSMO)
ferromagnet
$La_{0.7}Sr_{0.3}FeO_3$ (LSFO)
antiferromagnet

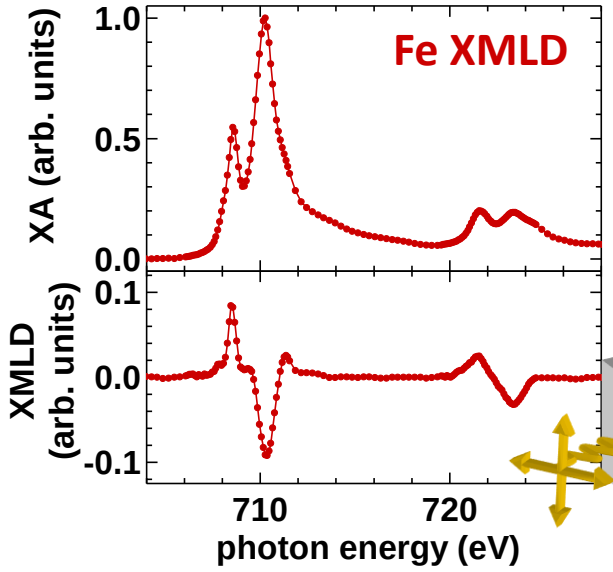

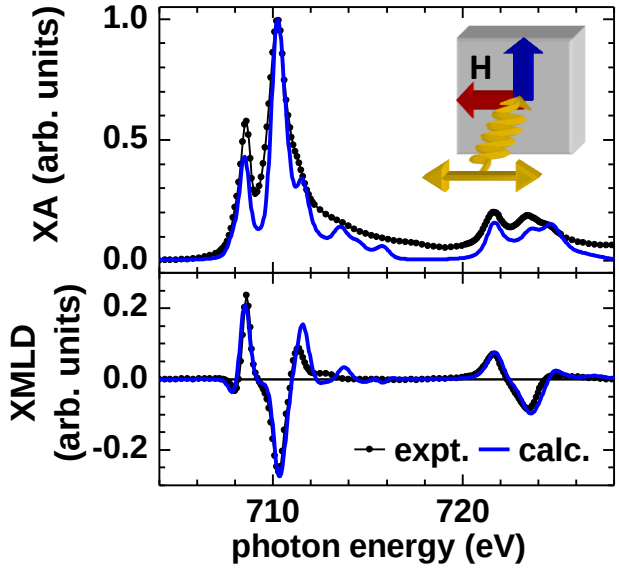

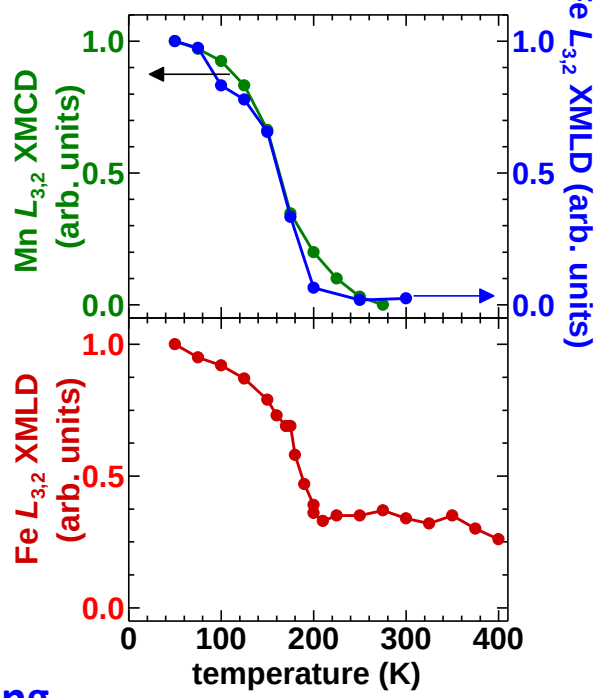

⇒ Perpendicular coupling at LSMO/LSFO interface

E. Arenholz *et al.*,
Appl. Phys. Lett. 94, 072503 (2009)

Planar Domain Wall

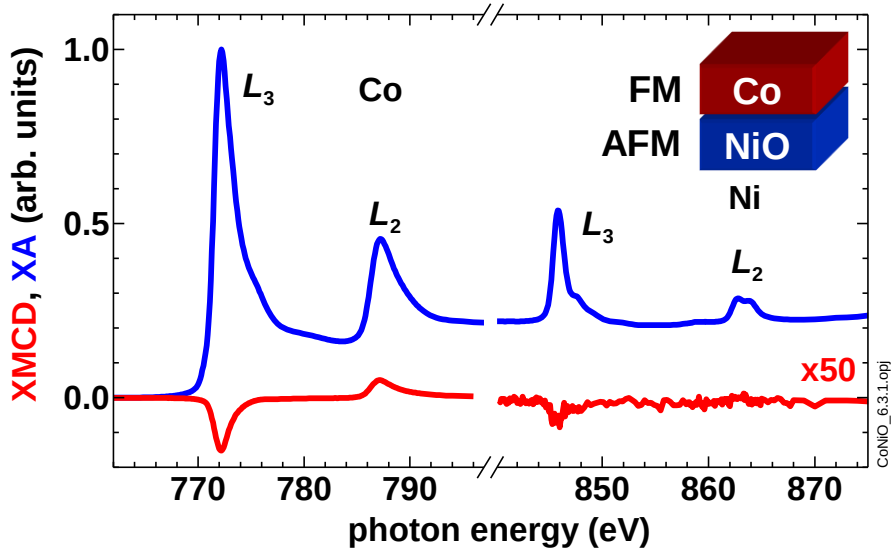

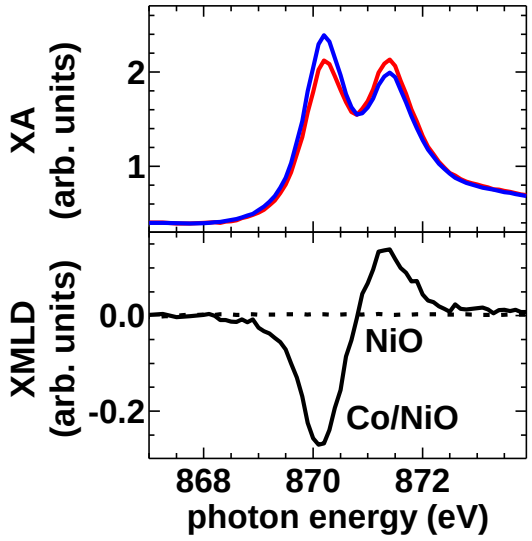

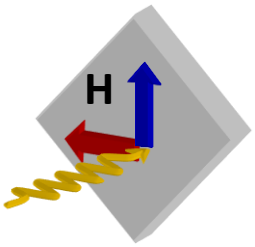

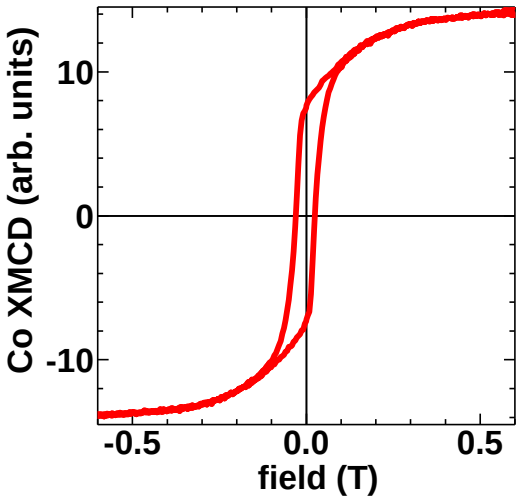

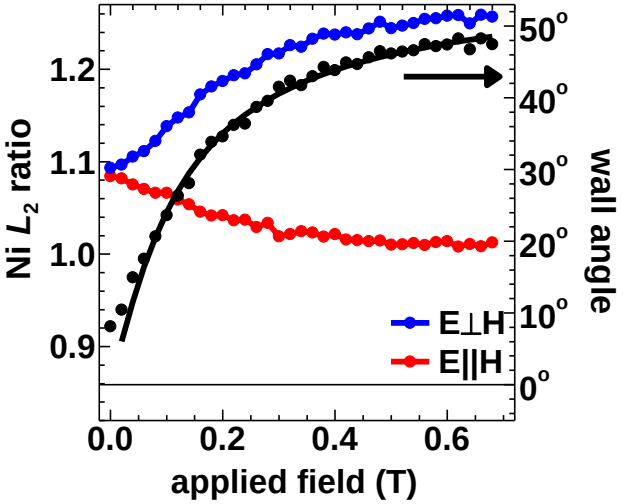

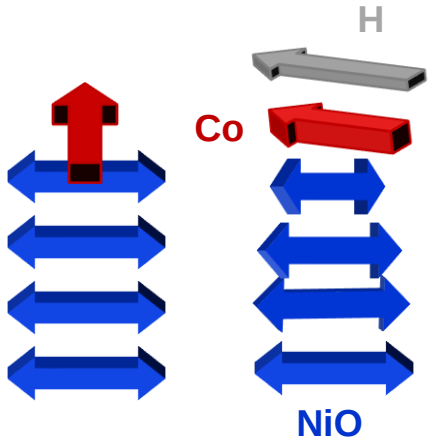

A. Scholl *et al.*,
Phys. Rev. Lett. 92, 247201 (2004)

MAGNETIC MICROSCOPY

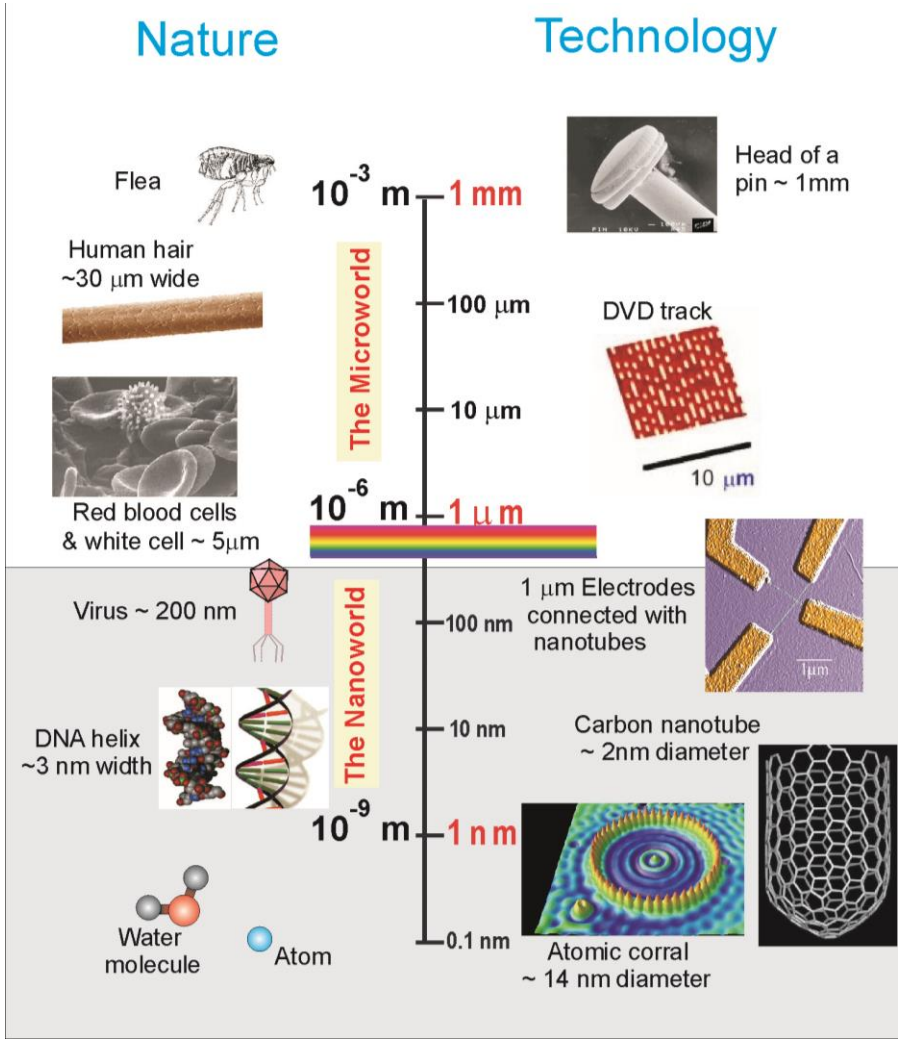

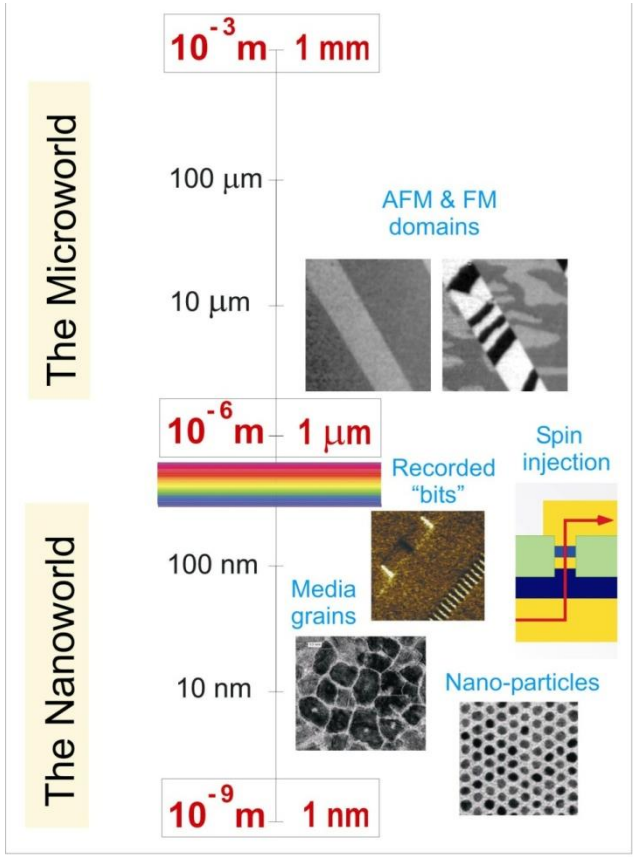

MAGNETIC MICROSCOPY

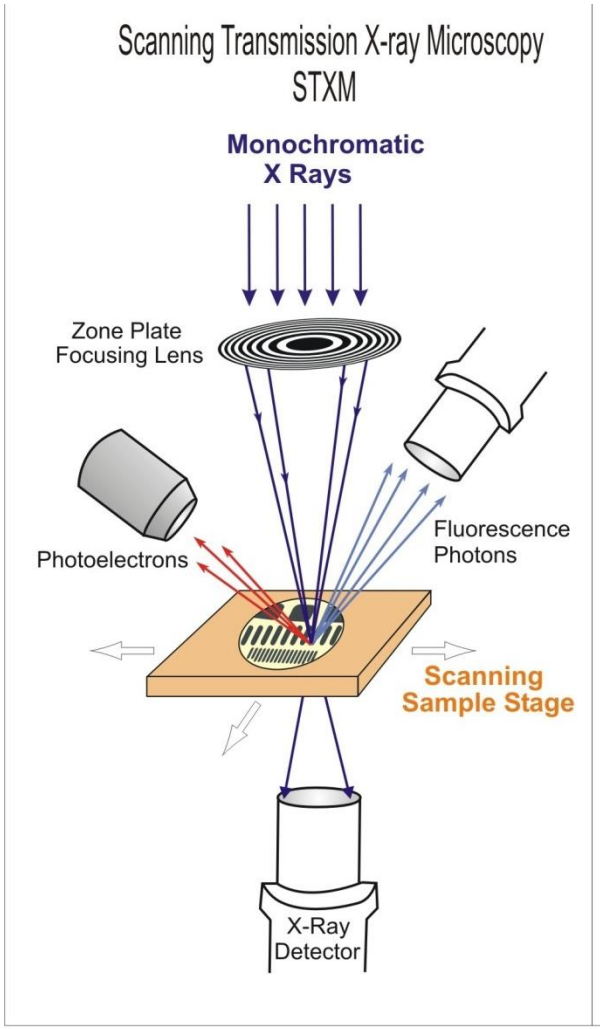

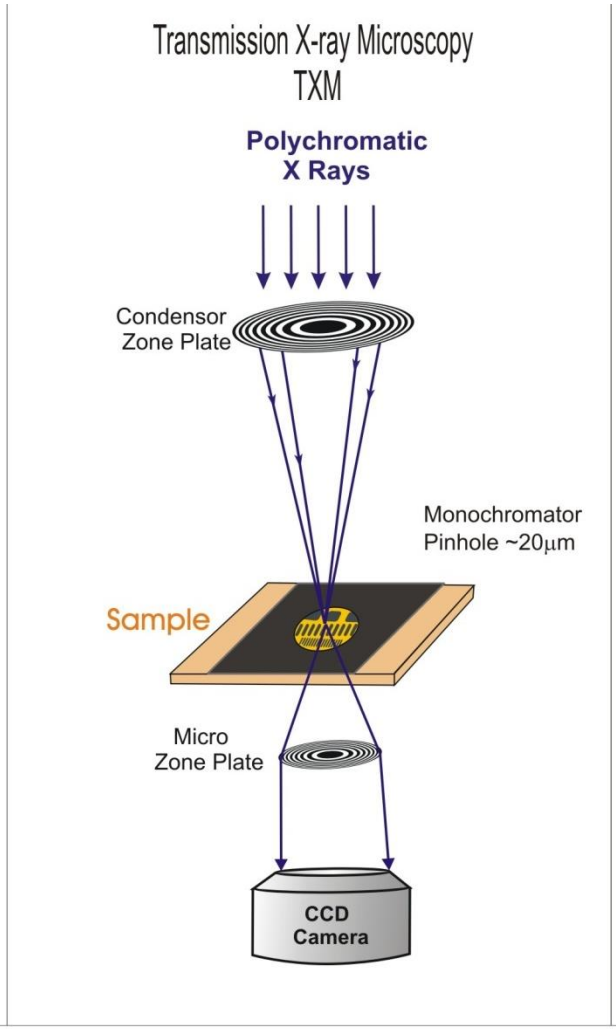

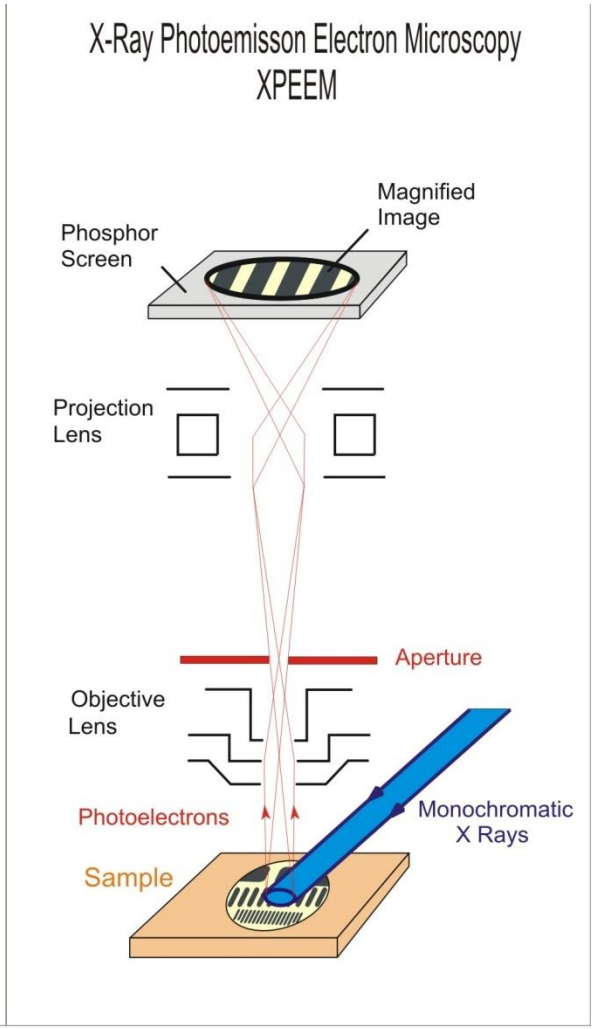

10-50 nm spatial resolution

J. Stöhr, H.C. Siegmann, Magnetism (Springer)

Imaging Magnetic Domains Using X-Rays

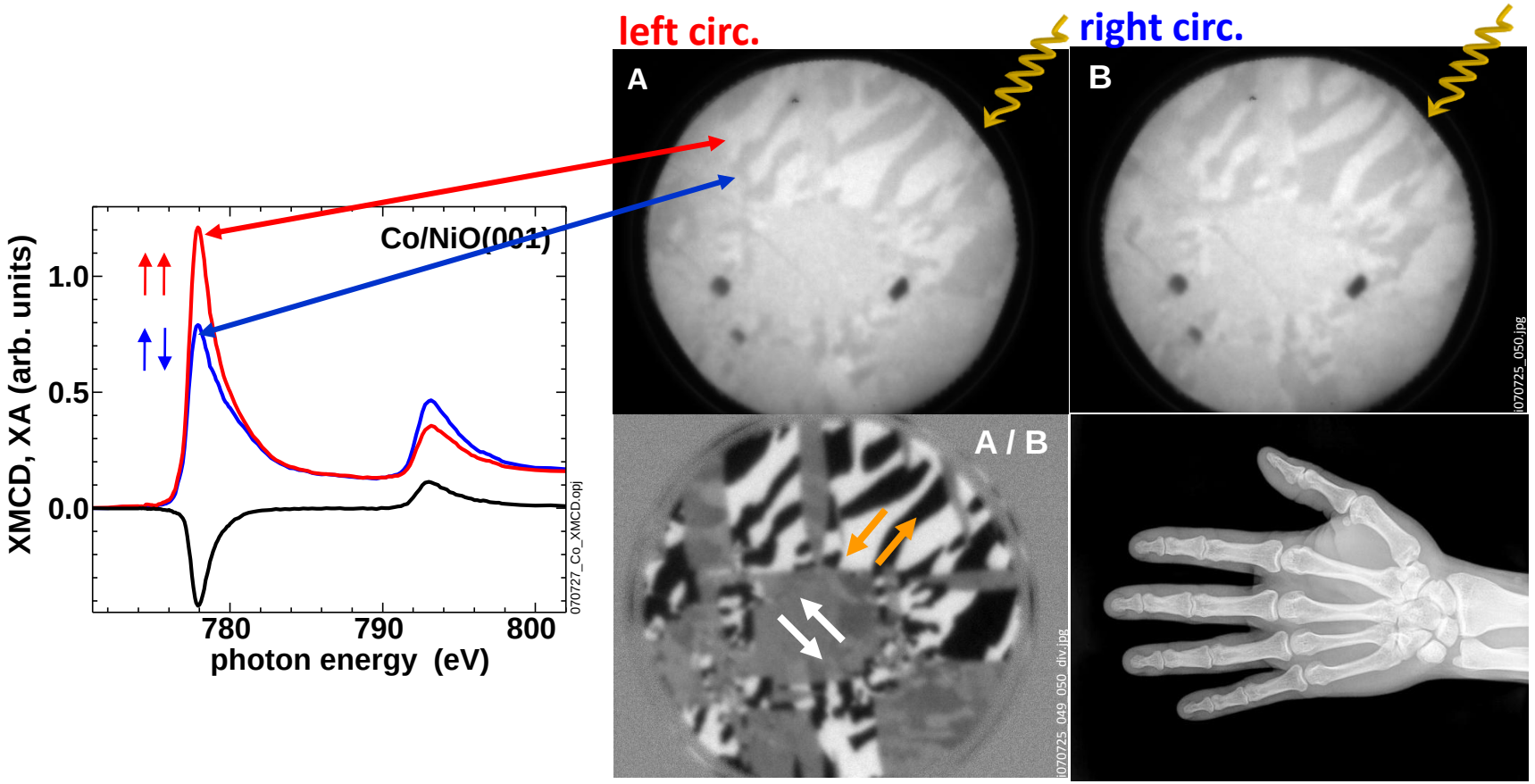

E. Arenholz *et al.*,
Appl. Phys. Lett. 93, 162506 (2008)

+ Images taken with left and right circularly polarized x-rays at photon energies with XMCD, i.e. Co L_3 edge, provide magnetic contrast and domain images.

Magnetic Coupling At Co/NiO Interface

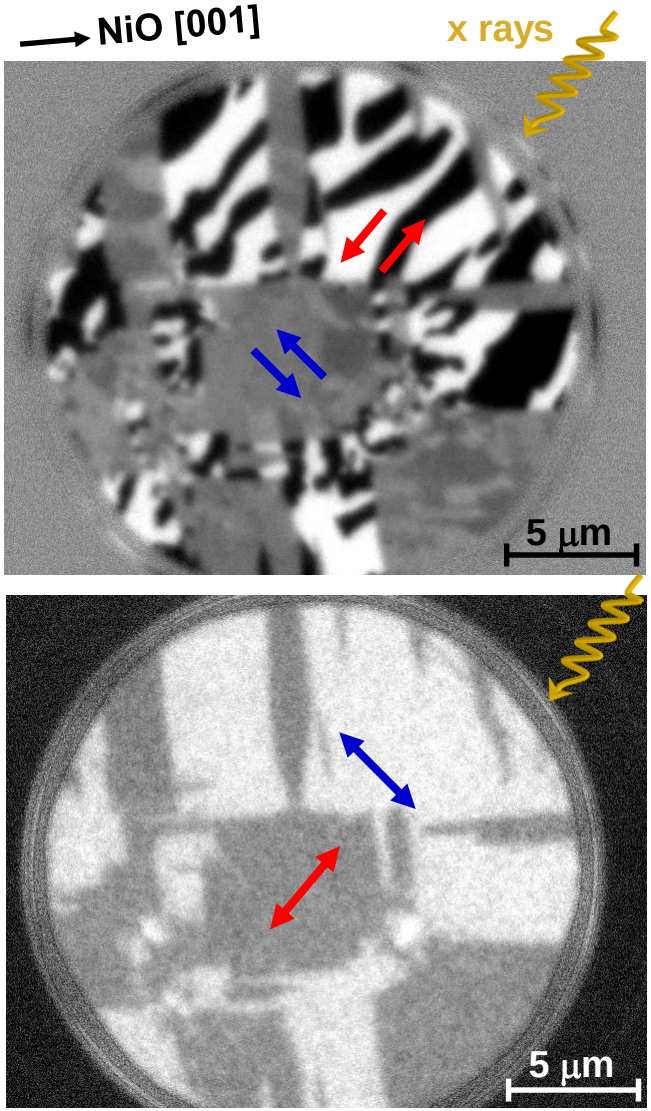

+ Taking into account the geometry dependence of the Ni XMLD signal

⇒ Perpendicular coupling of Co and NiO moments at the interface.

E. Arenholz *et al.*,
Appl. Phys. Lett. 93, 162506 (2008)

MAGNETIC VORTICES

+ First direct observation of vortex state in antiferromagnetic CoO and NiO disks in Fe/CoO and Fe/NiO bilayers using XMCD and XMLD.
+ Two types of AFM vortices:
  - conventional curling vortex as in ferromagnets
  - divergent vortex, forbidden in ferromagnets
  - thickness dependence of magnetic interface coupling

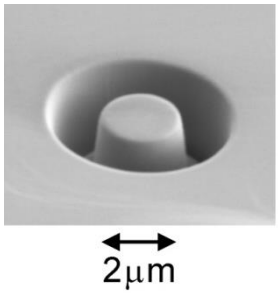

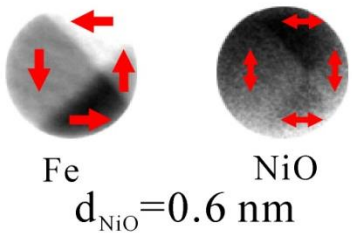

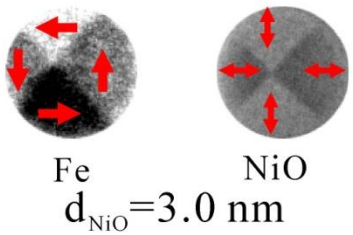

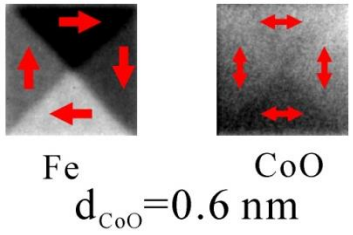

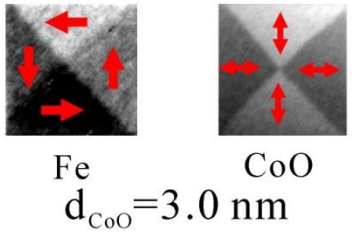

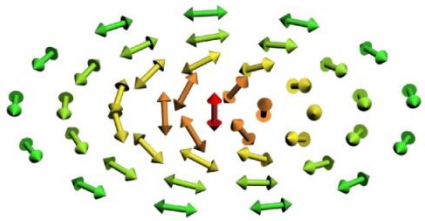

conventional curling vortex

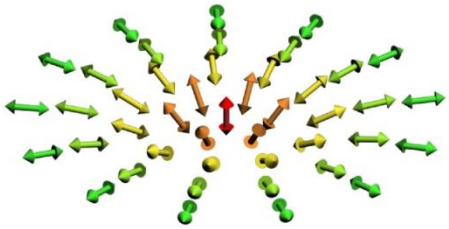

divergent vortex

J. Wu *et al.*, Nature Phys. 7, 303 (2011)

NANOSCALE MAGNETIC PHASES

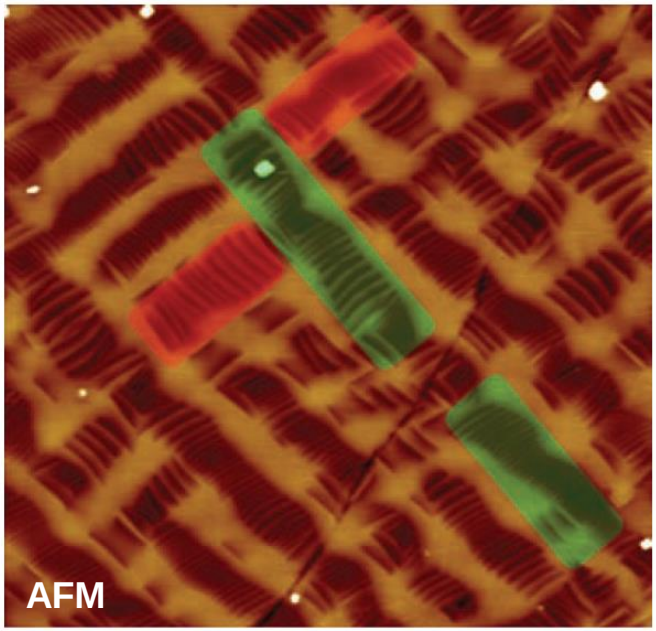

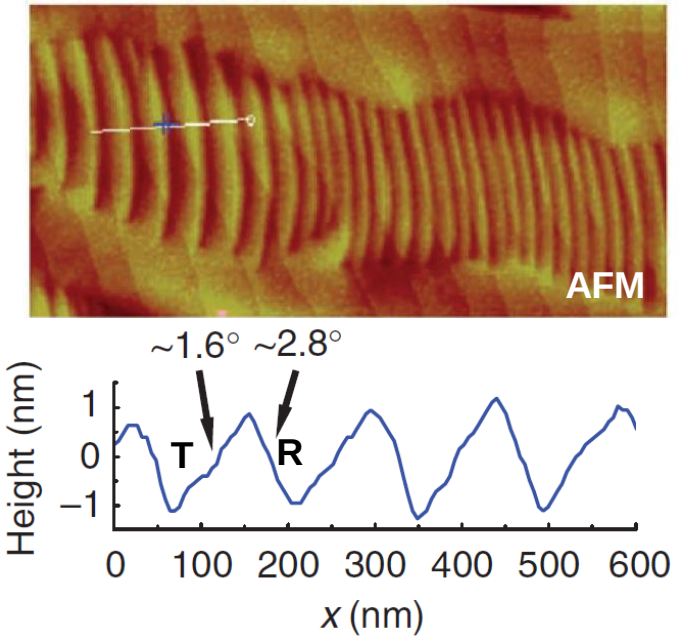

+ $BiFeO_3$ – multiferroic = ferroelectric + antiferromagnetic
+ Compressive strain on rhombohedral phase (R-phase) induced by substrate

⇒ tetragonal-like phase (T-phase)

+ Partial relaxation of epitaxial strain

⇒ Formation of a nanoscale mixture of T- and R-phases

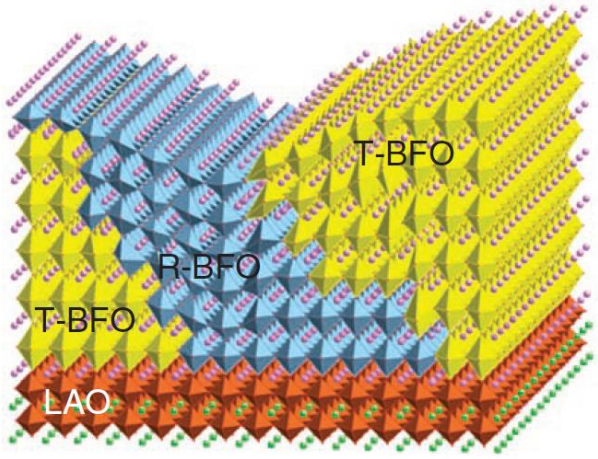

Q. He *et al.*, Nature Comm. 2, 225 (2011)

NANOSCALE MAGNETIC PHASES

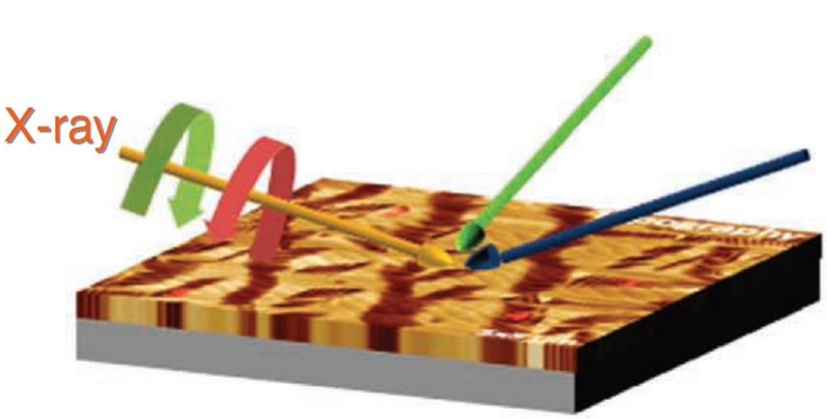

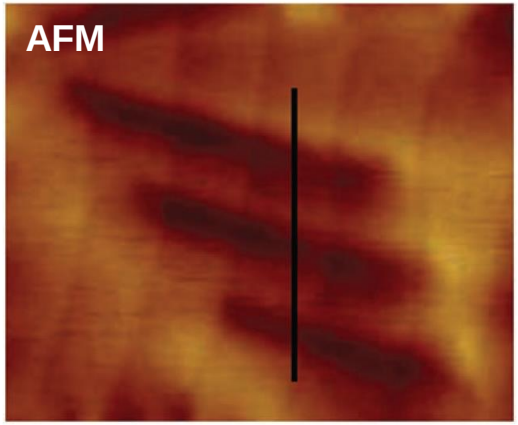

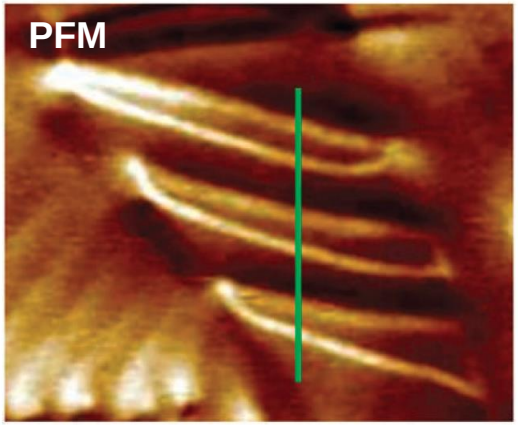

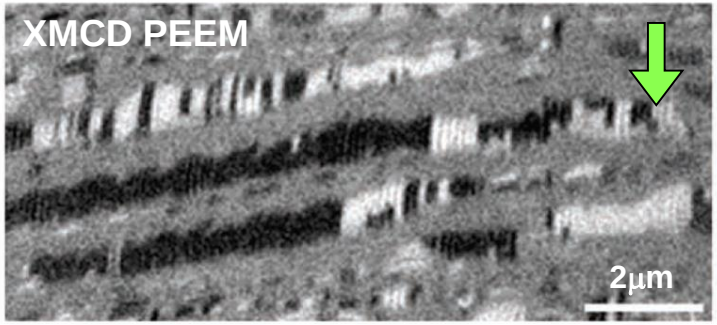

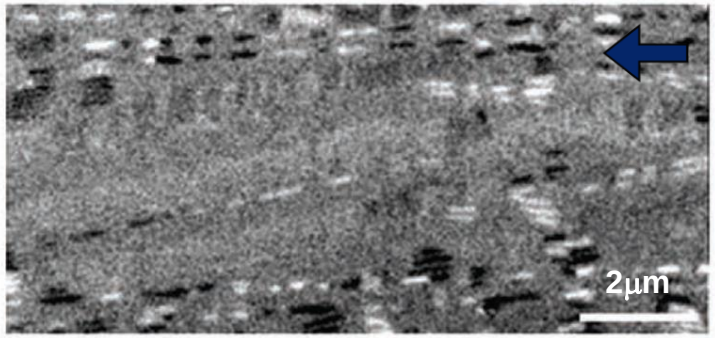

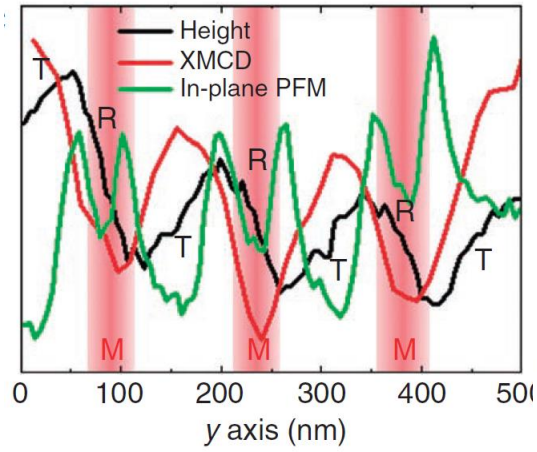

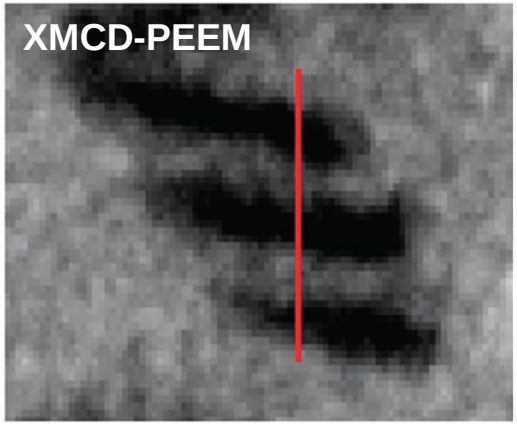

Q. He *et al.*,
Nature Comm. 2, 225 (2011)

+ **Highly distorted R-phase is the source of enhanced magnetic moment in the XMCD image.**

ULTRAFAST MAGNETISM

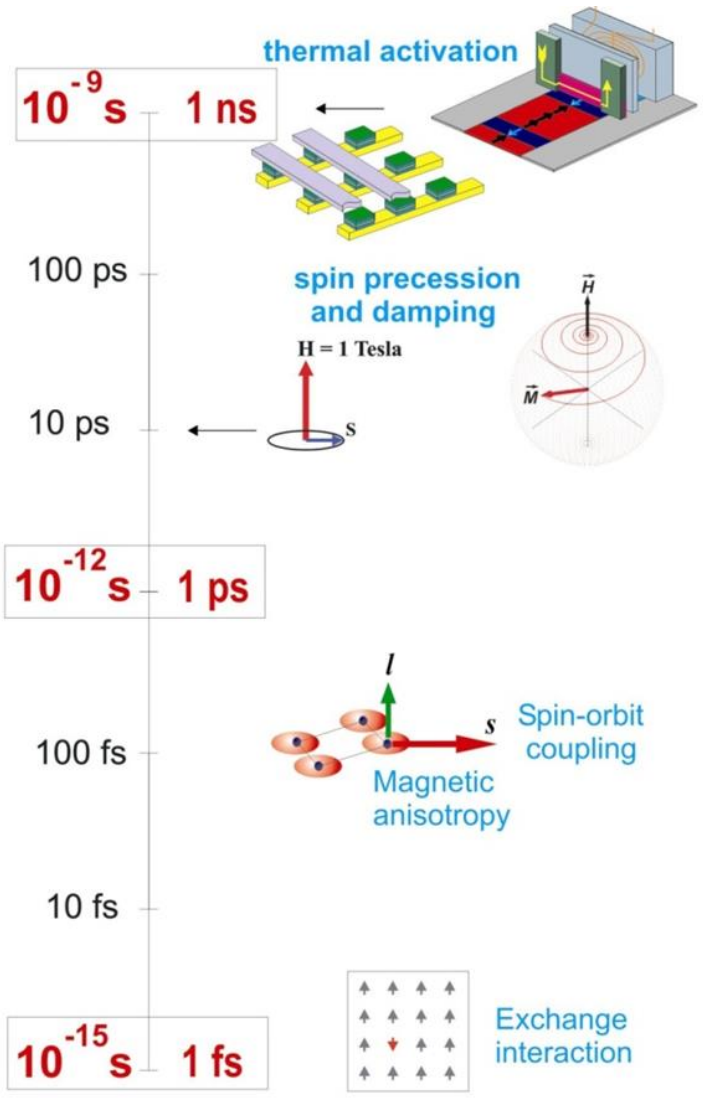

J. Stöhr, H.C. Siegmann, Magnetism (Springer)

+ Energy reservoirs in a ferromagnetic metal

+ Deposition of energy in one reservoir

⇒ Non-equilibrium distribution and subsequent relation through energy and angular momentum exchange

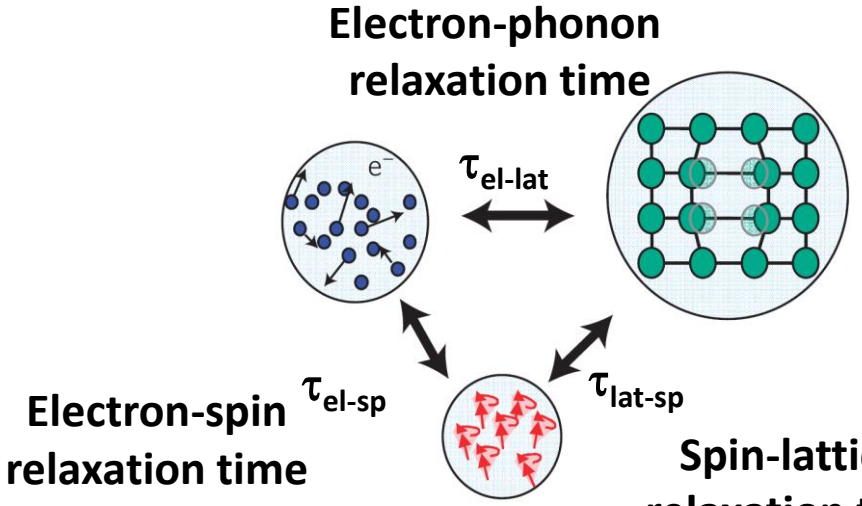

Ultrafast Dynamics Of Spin And Orbital Moments

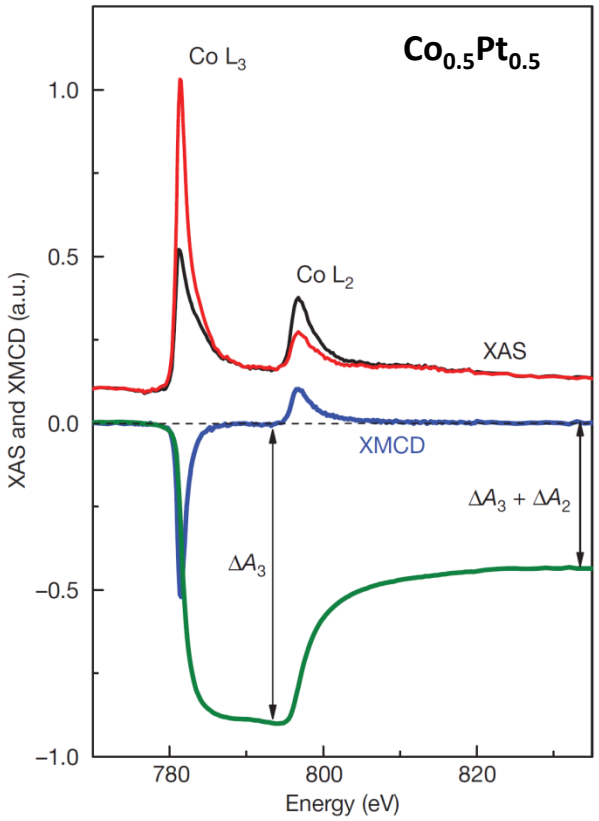

C. Boeglin, *et al.*,
Nature 465, 458 (2010)

+ Orbital (*L*) and spin (*S*) magnetic moments can change with total angular momentum is conserved.
+ Efficient transfer between *L* and S through spin–orbit interaction in solids
+ Transfer between *L* and *S* occurs on fs timescales.

+ $Co_{0.5}Pt_{0.5}$ with perpendicı magnetic anisotropy
+ 60 fs optical laser pulses change magnetization
+ Dynamics probed with XMCD using 120fs x-ray pulses

+ Linear relation connects Co L_3 and L_2 XMCD with L_z and S_z using sum rules

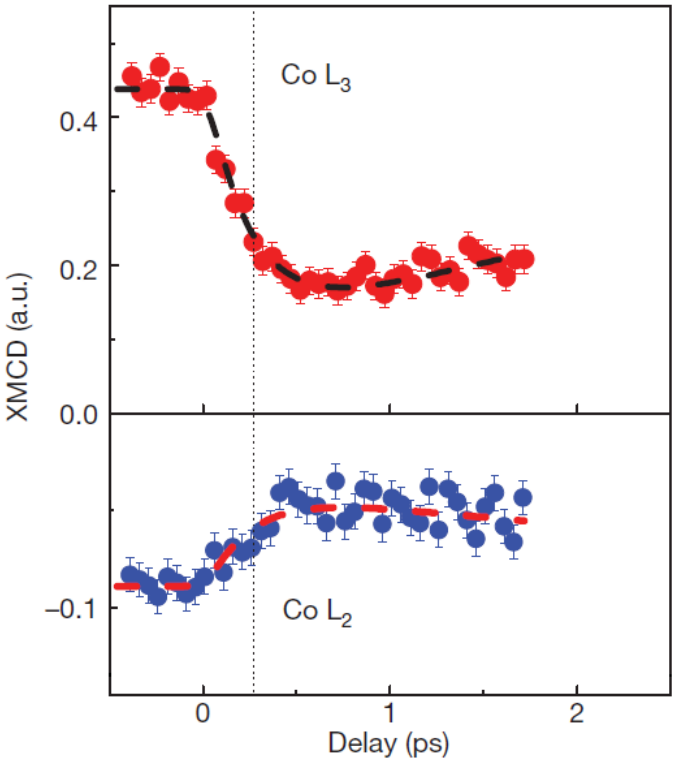

Ultrafast Dynamics Of Spin And Orbital Moments

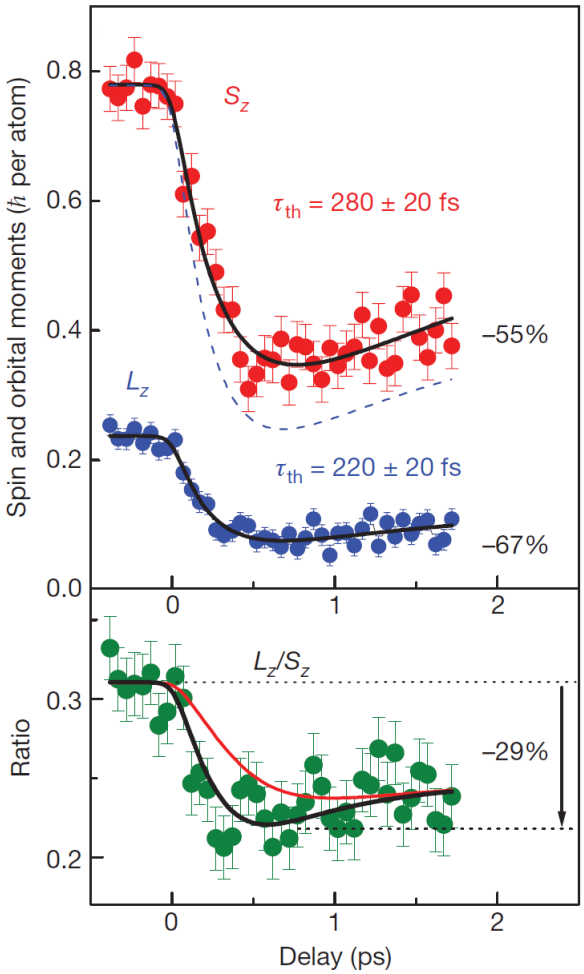

C. Boeglin, *et al.*,
Nature 465, 458 (2010)

+ **Thermalization: Faster decrease of orbital moment**
+ **Theory: Orbital magnetic moment strongly correlated with magnetocrystalline anisotropy**
+ **Reduction in orbital moment**
  ⇔ Reduction in magnetocrystalline anisotropy
+ **Typically observed at elevated temperatures in static measurements as well**

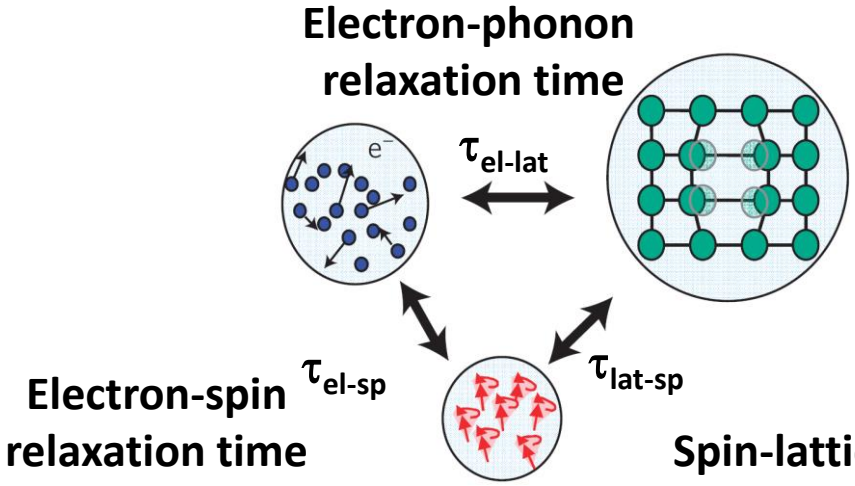

References And Further Reading

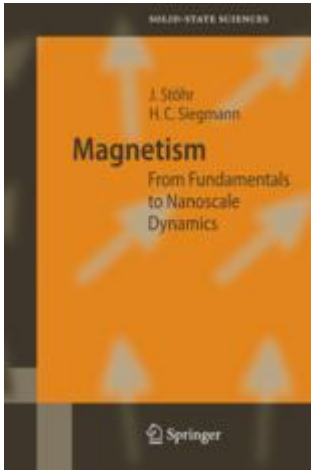

J. Stöhr, H.C. Siegmann
Magnetism– From Fundamentals to Nanoscale Dynamics
Springer